Elsevier Editorial System(tm) for BBA - Bioenergetics

Manuscript Draft

Manuscript Number:

Title: Subunit Asa1 spans all the peripheral stalk of the mitochondrial ATP synthase of the chlorophycean alga Polytomella sp.

Article Type: Regular Paper

Keywords: F1FO-ATP synthase peripheral-stalk;
dimeric mitochondrial complex V;
chlorophycean algae;
Chlamydomonas reinhardtii;
Polytomella sp.;
Asa subunits.

Corresponding Author: Prof. Diego Gonzalez-Halphen, Ph.D.

Corresponding Author's Institution: Instituto Fisiologia Celular, UNAM

First Author: Lilia Colina-Tenorio, Ph.D. student

Order of Authors: Lilia Colina-Tenorio, Ph.D. student; Héctor Miranda-Astudillo, Ph.D.; Araceli Cano-Estrada, Ph.D.; Miriam Vázquez-Acevedo, Chemist; Cardol Pierre, Ph.D.; Claire Remacle, Ph.D.; Diego Gonzalez-Halphen, Ph.D.

Abstract: Mitochondrial F1FO-ATP synthase of chlorophycean algae is isolated as a dimer. Besides the eight orthodox subunits (alpha, beta, gamma, delta, epsilon, OSCP, a and c), the enzyme contains nine atypical subunits (Asa1 to 9). These subunits build the peripheral stalk of the enzyme and stabilize its dimer structure. The location of the 60.6 kDa subunit Asa1 has been debated. On one hand, it was found in a transient subcomplex that contained membrane-bound subunits Asa1/Asa3/Asa5/Asa8/a (Atp6)/c (Atp8). On the other hand, Asa1 was proposed to form the bulky structure of the peripheral stalk that contacts the OSCP subunit in the F1 sector. Here, we over-expressed and purified the recombinant proteins Asa1 and OSCP and explored their interactions in vitro, using immunochemical techniques and affinity chromatography. Asa1 and OSCP interact strongly, and the carboxy-terminal half of OSCP seems to be instrumental for this association. In addition, the algal ATP synthase was partially dissociated at relatively high detergent concentrations, and an Asa1/Asa3/Asa5/Asa8/a/c10 subcomplex was characterized. Based on these results, a model is proposed in which Asa1 spans the whole peripheral arm of the enzyme, from a region close to the matrix-exposed side of the mitochondrial inner membrane to the F1 region where OSCP is located. We also suggest which residues in Asa1 and OSCP may mediate their interaction. Subunit b is the main component of the peripheral stalk of orthodox mitochondrial enzymes. Although no obvious sequence similarity exists between Asa1 and subunit b, both subunits probably play a similar structural role.

Suggested Reviewers: Norbert A. Dencher Ph.D.
Professor, Faculty of Chemistry, Technische Universitat Darmstadt
norbert.dencher@physbiochem.tu-darmstadt.de

Expert in ATP synthases

Volker Muller Ph.D.
Professor, Molecular Microbiology and Bioenergetics, Johann Wolfgang Goethe-Universitat Frankfurt
vmueller@bio.uni-frankfurt.de
Expert in Archaea A1Ao-ATP synthases

Steven B. Vik Ph.D.
Professor, Biological & Life Sciences, Southern Methodist University
svik@smu.edu
Expert in bacterial ATP synthases.

Stanley D. Dunn Ph.D.
Professor, Biochemistry, Western University, Canada
sdunn@uwo.ca
Expert on the peripheral arm of bacterial ATP synthases.

Thomas M. Duncan Ph.D.
Professor, Biochemistry and Molecular Biology, Upstate Medical University
duncant@upstate.edu
Expert in bacterial ATP synthases.

Cover Letter

INSTITUTO DE FISIOLOGÍA CELULAR
DEPARTAMENTO DE GENÉTICA MOLECULAR
UNIVERSIDAD NACIONAL
AUTÓNOMA DE MÉXICO
Apdo. Postal 70-243
04510 México D.F.
Dr. Diego González-Halphen
Tel: (5255) 5622-56-20
Fax: (5255) 5622-56-11
Correo electrónico: dhalphen@ifc.unam.mx

Mexico City, August 24, 2015

Editor, BBA-Bioenergetics

Sir,

Please find attached the manuscript entitled “Subunit Asa1 spans all the peripheral stalk of the mitochondrial ATP synthase of the chlorophycean alga *Polytomella* sp.” from authors Lilia Colina-Tenorio et al.

In the last years, it has become increasingly clear that ATP synthases may exhibit peripheral stalks with different structures and architectures. Such is the case of the ciliate *Tetrahymena*, the trypanosomatid *Trypanosoma*, and the chlorophycean algae *Chlamydomonas* and *Polytomella*. Undoubtedly, the best atypical enzyme characterized to date from the structural and the biochemical points of view is the later one. The algal enzyme contains nine atypical subunits (Asa1 to Asa9) that constitute a robust peripheral stalk as seen in electron microscopy studies. In this work, we overexpressed and purified subunits Asa1 and OSCP and explored their interactions in vitro, using immunochemical techniques, blue native electrophoresis and affinity chromatography. Based on the obtained results we propose a model in which Asa1 spans the peripheral arm of the algal ATP synthase from a region close to the membrane to OSCP, substituting subunit *b* found in orthodox enzymes.

We believe this work brings new insights on the structure of the peripheral stalk in algal mitochondrial ATP synthases and that it may be of interest to several colleagues of the Bioenergetics community. We hope you may consider this manuscript to be published in BBA Bioenergetics.

Yours sincerely,

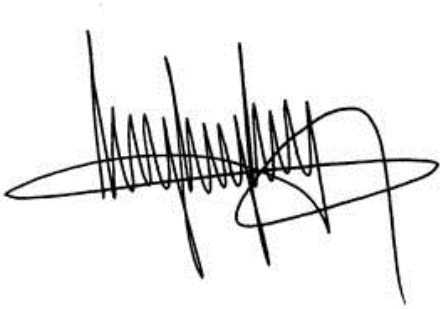

Diego González-Halphen, Ph.D.

HIGHLIGHTS

- We studied the interactions of the recombinant proteins Asa1 and OSCP of the algal ATP synthase.
- The carboxy-terminal half of OSCP seems to be instrumental for the interaction with Asa1.
- Asa1 was also identified in a subcomplex containing several membrane-bound subunits.
- A SDS-resistant *c*-ring was identified in the algal ATP synthase.
- Asa1 may span the whole peripheral arm substituting for orthodox subunit *b*.

Subunit Asa1 spans all the peripheral stalk of the mitochondrial ATP synthase of the chlorophycean alga *Polytomella* sp.

Lilia Colina-Tenorio[1], Héctor Miranda-Astudillo[1*], Araceli Cano-Estrada [1], Miriam Vázquez-Acevedo[1], Pierre Cardol[2], Claire Remacle[2] and Diego González-Halphen[1]

[1]Instituto de Fisiología Celular, Universidad Nacional Autónoma de México, México D.F. (Mexico)

[2]Genetics and Physiology of Microalgae, Department of Life Sciences, University of Liège, B-4000 Liège (Belgium).

Suggested running head: Asa1 subunit of algal ATP synthase.

Corresponding author: Diego González-Halphen, Departamento de Genética Molecular, Instituto de Fisiología Celular, UNAM, Apartado Postal 70-600, Delegación Coyoacán, 04510 México D.F., Mexico; Tel. 5255 5622-5620; Fax. 5255 5622-5611; E-mail: dhalphen@ifc.unam.mx

Abstract

Mitochondrial F_1F_O-ATP synthase of chlorophycean algae is isolated as a dimer. Besides the eight orthodox subunits (alpha, beta, gamma, delta, epsilon, OSCP, *a* and *c*), the enzyme contains nine atypical subunits (Asa1 to 9). These subunits build the peripheral stalk of the enzyme and stabilize its dimer structure. The location of the 60.6 kDa subunit Asa1 has been debated. On one hand, it was found in a transient subcomplex that contained membrane-bound subunits Asa1/Asa3/Asa5/Asa8/*a* (Atp6)/*c* (Atp8). On the other hand, Asa1 was proposed to form the bulky structure of the peripheral stalk that contacts the OSCP subunit in the F_1 sector. Here, we over-expressed and purified the recombinant proteins Asa1 and OSCP and explored their interactions *in vitro*, using immunochemical techniques and affinity chromatography. Asa1 and OSCP interact strongly, and the carboxy-terminal half of OSCP seems to be instrumental for this association. In addition, the algal ATP synthase was partially dissociated at relatively high detergent concentrations, and an Asa1/Asa3/Asa5/Asa8/a/c_{10} subcomplex was

characterized. Based on these results, a model is proposed in which Asa1 spans the whole peripheral arm of the enzyme, from a region close to the matrix-exposed side of the mitochondrial inner membrane to the F_1 region where OSCP is located. We also suggest which residues in Asa1 and OSCP may mediate their interaction. Subunit *b* is the main component of the peripheral stalk of orthodox mitochondrial enzymes. Although no obvious sequence similarity exists between Asa1 and subunit *b*, both subunits probably play a similar structural role.

KEY WORDS: F_1F_O-ATP synthase peripheral-stalk; dimeric mitochondrial complex V; chlorophycean algae; *Chlamydomonas reinhardtii*; *Polytomella* sp.; Asa subunits.

1. Introduction

Mitochondrial F_1F_O-ATP synthase (complex V) is an oligomeric membrane complex that works as a rotary motor driven by the electrochemical proton gradient generated by the respiratory chain. In fungi and animals, the enzyme comprises distinct multi-subunit domains: a soluble fraction (F_1) bearing the catalytic core [α_3/β_3] and a central rotor-stalk [$\gamma/\delta/\varepsilon$], a membrane bound sector F_O that translocates protons [*a*/$c_{9\text{-}14}$ ring], a peripheral stator-stalk [OSCP/b/d/F6] and a dimerization module [A6L/e/f/g] [1].

Protons are translocated through subunit *a* and the *c*-ring, which in turn drives rotation of the central rotor stalk. The gamma subunit extends from the matrix-exposed side of the *c*-ring and inserts into the F_1 catalytic core, inducing conformational changes in the α_3/β_3 subunits that lead to ATP synthesis [2]. The main function of the peripheral stator-stalk is to hold the F_1 sector against the movement of the rotor stalk [3]. In the inner mitochondrial membrane, the ATP synthase forms oligomeric structures [4], stabilized by the dimerization module A6L/e/f/g, that are responsible for the overall architecture of the mitochondrial cristae [5]. Subunits *b* (Atp4), *d*, F6, A6L, *e*, *f* and *g* are not common to all mitochondrial ATP synthases, since several enzymes exhibit different overall architecture and subunit composition. Such is the case of the ATP synthases from the ciliate *Tetrahymena thermophila* [6], the trypanosomatid *Trypanosoma brucei* [7], the euglenoid *Euglena gracilis* [8], and the chlorophycean algae like *Chlamydomonas reinhardtii* and *Polytomella* sp. [9].

The mitochondrial F_1F_O-ATP synthase of chlorophycean algae is isolated as a highly stable dimer of 1600 kDa after solubilization with detergents such as n-dodecyl-β-D-maltoside [10]. As in all known eukaryotes, the rotary and catalytic cores of the algal enzyme are formed by the eight conserved subunits α, β, γ, δ, ε, *a* (Atp6), *c* (Atp9), and OSCP [11]. Nevertheless, nine non-conventional subunits (Asa1 to Asa9), unique to the mitochondrial ATP synthases of chlorophycean algae, are also constituents of the enzyme. Some Asa subunits form the robust peripheral stalk observed in several electron microscopy analyses of the isolated enzyme [12-16] while others (Asa6, Asa7 and Asa9) may participate in the dimerization of the enzyme [17-20].

The neighboring interactions between Asa subunits in the ATP synthase of the colorless chlorophycean alga *Polytomella* sp. have been addressed in the past using several experimental approaches: characterizing enzyme subcomplexes generated by heat dissociation [9, 17], defining near-neighbor relationships of subunits using cross-linking agents [14] and identifying protein-protein interactions in vitro employing recombinant subunits [20]. Thus, successive models for the topological disposition of the Asa polypeptides in the peripheral arm of the enzyme have been proposed [9, 17, 14, 20]. An electron cryomicroscopy map at 7.0 Å overall resolution of the *Polytomella* dimeric ATP synthase revealed that the peripheral stalks consist of several entwined alpha-helices that give rise to a solid scaffold [16] that is strikingly more robust that the peripheral arm of enzymes from other biological sources, including bovine [21, 22], yeast [23], spinach chloroplasts [24], and *Escherichia coli* [25]. Although many Asa subunits are thought to be localized in the peripheral stator stalk, the position of the Asa1 subunit remains controversial. On one hand, Asa1 was identified in a subcomplex that contained subunits Asa3/Asa5/Asa8/*a*/*c* and that appeared transiently during a time course of heat treatment of the enzyme before it further dissociated into its free components [9]. This result suggested that Asa1 may be interacting closely with subunits which are known to be membrane-bound, i.e. *a* (five transmembrane stretches or TMS), Asa8 (one TMS) and *c* (two TMS). On the other hand, Asa1 was proposed to form a bulky structure near the catalytic region of the enzyme,

close to OSCP [17] based on electron microscopy studies [12] and on the fact that Asa1 behaved as an extrinsic membrane protein. Here, we studied the disposition of Asa1 in the peripheral stalk and suggest that Asa1 spans the whole peripheral stalk from the matrix-exposed side of the inner mitochondrial membrane to the F_1 region where OSCP resides. We propose that chlorophycean Asa1, although not anchored directly to the lipid bilayer, is the structural equivalent of subunit *b* (Atp4) found in the mitochondrial ATP synthases of yeasts, mammals and green plants with an orthodox subunit composition.

2. Materials and methods

2.1 Algal strains and growth conditions

Polytomella spec. (Strain number 198.80, isolated by E.G. Pringsheim), identical to *Polytomella parva*, was originally obtained from the Culture Collection of Algae (University of Göttingen, Germany). Cells were grown for 48 h at room temperature in 2.5-liter wide-bottom culture flasks without shaking, in a medium containing 4 g/l of sodium acetate, 2 g/l of Bacto™ Tryptone (Becton, Dickinson and Co.) and 2 g/l of Bacto™ Yeast Extract (Becton, Dickinson and Co.), supplemented with 10 μg/ml of vitamin B1 (thiamine) and 0.5 μg/ml of vitamin B12 (cobalamin).

2.2 Polytomella mitochondrial ATP synthase purification

Polytomella sp. cells were collected by centrifugation at 7,500 *g* for 10 min and washed with sucrose buffer (20 mM Tris, 0.37 M sucrose, 4 M potassium EDTA, pH 7.4). The resulting pellet was suspended in the same buffer (80-100 mL). The cells were broken using a Potter homogenizer, centrifuged at 7,500 *g* for 15 min and the supernatant was recovered. The unbroken cell pellet was treated again as described above; both supernatants were mixed and centrifuged at 17,500 *g* for 20 min to recover the mitochondria pellet, which was suspended in a small volume of sucrose buffer and stored at -70 ºC until used. The mitochondria (250 mg of protein) were diluted to a final concentration of 10 mg/mL with

solubilization buffer (50 mM Tris, 100 mM NaCl, 1 mM $MgSO_4 \cdot 7H_2O$, 10% glycerol, 1 mM PMSF, 50 μg/mL TLCK, pH 8.4) and were incubated with n-dodecyl β-D-maltoside (2 mg of detergent per mg of protein) under mild agitation for 30 min at 4°C. The sample was centrifuged at 90,000 *g* for 20 min, the supernatant was recovered, diluted 3 times with loading buffer (50 mM Tris, 1 mM $MgSO_4 \cdot 7H_2O$, 10% glycerol, 1 mM PMSF, 50 μg/mL TLCK, 0.01% n-dodecyl β-D-maltoside pH 8.4) and loaded to a Source 15Q 10/100 GL column (CV 8 mL) (GE Healthcare) with a 1 mL/min flow. The column was washed with 75 mM NaCl and then eluted with a linear NaCl gradient (75-250 mM) in the same buffer. Two milliliter fractions were collected and analyzed by Tricine-SDS-PAGE. The fractions enriched with ATP synthase were pooled and concentrated to a volume of 4 mL using a Amicon Ultra 15 centrifugal filter 100,000 NMWL. Glycerol and ATP were added to final concentrations of 30% and 1 mM, respectively, and the sample was further concentrated to a final volume of 400 μL. This sample was injected to a Superose 6 10/300 GL (CV 24 mL) (GE Healthcare) previously equilibrated with Superose buffer (50 mM Tris, 150 mM NaCl, 1 mM $MgSO_4 \cdot 7H_2O$, 10% glycerol, 1 mM PMSF, 50 μg/mL TLCK, 0.01% n-dodecyl β-D-maltoside, 2 mM ATP, pH 8.4). The elution was carried out at a 0.25 mL/min flow. Fractions were collected (500 μL each) and analyzed by SDS-PAGE and BN-PAGE. The purified ATP synthase was aliquoted and stored at -70 ºC until used.

2.3 Protein analysis

Denaturing gel electrophoresis was carried out in a Tricine-SDS-PAGE system [26], and when indicated, it was followed by 2D-Glycine-SDS-PAGE analysis [27]. Blue native polyacrylamide gel electrophoresis (BN-PAGE) was carried out as previously described [28]. When indicated, 1D-BN-PAGE was followed by 2D-Tricine-SDS-PAGE [26]. Protein concentration was determined as published [29].

2.4 Dissociation of the ATP synthase into subcomplexes

The purified algal ATP synthase (100 μg of protein) was incubated for 24 h at 4 °C under mild agitation in the presence of 3.0 % lauryl maltoside and the solubilized sample subjected to BN-PAGE in 4-12% gradient acrylamide gels. The resulting lane of interest was excised and incubated in the presence of 1.0 % SDS and 1.0 % beta-mercaptoethanol for 15 min and then subjected to 2D Tricine-SDS-PAGE in 14 % acrylamide gels.

2.5 Cloning of the cDNAs encoding subunits of the ATP synthase of Polytomella sp. in expression vectors

The cDNAs of *Asa1*, *OSCP* and *OSCPΔC* were PCR-amplified from a *Polytomella* sp. cDNA library cloned in λ-ZapII phages [30] using specific oligonucleotide primers: for Asa1, forward 5'-GCGGCATGCGCTAGCTACCTTGCCCCCCTCCGCTCTGAT - 3' and reverse 5'- GCGCTGCAGGCGGCCGCTTAGTTACCGTTGACGAGATC - 3'; for OSCP, forward 5'- GCGGGATCCCATATGGCTGCCCAGGCTGAGCTCAAG - 3' and reverse 5'-GCGCTGCAGGTCGACAACGAACTAATTTAAATAGAAAGA - 3' and for OSCPΔC, forward 5'-GCGGGATCCCATATGGCTGCCCAGGCTGAGCTCAAG - 3' and reverse 5'-GCGCTGCAGGTCGACCTAAACCTCCTTCTTGTGAGCGAG - 3'. The *Asa1* amplification product was cloned into a pET28a vector using the restriction sites *Nhe*I and *Bam*HI. This vector adds a hexa-histidine tag (6His-tag) to the N-terminus of the expressed protein. The OSCP amplification product was cloned into a pET28a vector as well as into a pET3a vector using the restriction sites *Nhe*I and *Sal*I. The *OSCPΔC* product was obtained using the same forward primer that for OSCP and the reverse primer 5'-GCGCTGCAGGTCGACCTAAACCTCCTTCTTGTGAGCGAG - 3'. The *OSCPΔC* was cloned into pET28a using the restriction sites *Nhe*I and *Sal*I.

2.6 Overexpression of recombinant proteins

Competent *E. coli* BL21 Codon Plus (DE3) RIL cells (Agilent Technologies) were transformed with the construct of interest. Cells were grown in LB medium containing 64 μg/mL chloramphenicol and one of the following antibiotics: 50 μg/mL kanamycin for the pET28a vector or 100 μg/mL ampicillin for the pET3a vector. The overexpressed subunits were the complete Asa1 subunit (GenBank: AJ558193.2), the complete OSCP subunit (GenBank: GQ422707.1) and the N-terminal region of OSCP (OSCP-ΔC, approximately 13.5 kDa, comprising residues 5 to 126 of OSCP).

2.7 Purification of proteins

Bacterial inclusion bodies (ICBs) retaining the overexpressed recombinant proteins were isolated, washed with detergent and stored as previously described [20]. The recombinant polypeptides Asa1, Asa1-6H, OSCP-6H and OSCPΔC-6H were purified under denaturing conditions using affinity chromatography. The ICBs were solubilized in PBS buffer (50 mM NaH_2PO_4, 500 mM NaCl, pH 7.8) containing 8.0 M urea with mild agitation at 4 ºC during 8 h. The insoluble material was removed by centrifugation at 17,500 *g* for 10 min. The sample was diluted with PBS buffer to a final concentration of 4.0 M urea; imidazole was added to a final concentration of 10 mM from a 1.0 M stock solution. Then the sample was loaded on a 5 mL HisTrap FF crude column (GE Healthcare Life Sciences) equilibrated with PBS buffer containing 4.0 M urea. The column was washed with 30 mM imidazol and the proteins were eluted with a 30-500 mM imidazole linear gradient. The fractions obtained from the elution were analyzed by Tricine SDS-PAGE and those enriched with the recombinant protein of interest were pooled, concentrated, and stored at -70 °C until used. The ICBs containing untagged Asa1 were solubilized as described above. The resulting sample was dialyzed overnight against PBS buffer with 0.5 M urea, 500 mM NaCl, 2% glycerol and 0.1 % Tween 20. The aggregated material was removed by centrifugation at 17,500 *g* for 10 min and the supernatant was dialyzed (4 h) against the same buffer containing 200 mM NaCl, centrifuged at 17,500 *g* for 10 min and loaded to a 8 ml Source 15Q 10/100 column (GE Healthcare Sciences).

The protein was recovered after applying a 200-500 mM NaCl linear gradient; the enriched fractions were pooled, concentrated and stored at -70°C until used. The solubilized untagged OSCP inclusion bodies were dialyzed overnight against a buffer containing 20 mM MES, 2.0 % glycerol, 0.05% Tween 20, 1 mM EDTA, 1 mM DTT, pH 6.0. The recovered sample was centrifuged at 17,000 g for 10 min and the supernatant was loaded to a DEAE Sepharose FF column (24 mL) equilibrated with the same buffer. The protein was eluted with a 0-1.0 M NaCl linear gradient (10 column volumes). The eluted fractions were analyzed by Tricine-SDS-PAGE and the enriched fractions were pooled, concentrated and stored at -70°C until used.

2.8 Antibody production and immunoblotting

Antibodies were generated against subunits Asa1 and against OSCP. For this purpose, the polypeptides of the algal ATP synthase (50 µg of protein per lane) was resolved by Tricine-SDS-PAGE (14% acrylamide) in the presence of Serva Blue G as previously described [31]. The subunits of interest were excised from the gel, grinded in a mortar in the presence of 20 mM Tris (pH 7.0), mixed with Freund's complete adjuvant and injected into rabbits. The presence of antibodies in the sera was ascertained by Western blot analysis carried out as previously described [32]. For Western blots, goat anti-rabbit IgG conjugated with alkaline phosphatase (1:3000 for 2 h) was used, and color developed with nitro-blue tetrazolium chloride and 5-bromo-4-chloro-3'-indolylphosphate p-toluidine salt. Western blot mages were captured in a HP Scanjet G4050.

2.9 Protein-protein interaction assayed by Far-Western analysis

Far-Western analysis was carried out according as previously described [33] with modifications [20]. Purified *Polytomella* sp. ATP synthase was subjected to Tricine-SDS-PAGE and transferred to nitrocellulose membranes. The membranes containing the denatured enzyme were blocked with a 5.0 % powdered milk suspension overnight and then incubated for 4 hours in the presence of the externally-added protein of interest in increasing concentrations in the

corresponding buffer (for Asa1: PBS buffer with 0.5 M urea, 500 mM NaCl, 2.0 % glycerol and 0.05% Tween 20, pH 7.8; and for OSCP: MES 20 mM, 500 mM NaCl, 2.0 % glycerol, and 0.05% Tween 20, pH 6.0) supplemented with 1.0 % powdered milk. Protein bands were visualized by Ponceau S red staining (0.1% in 5% acetic acid) for 10 minutes. The membranes were washed two times with the same buffer. The protein of interest was recognized using a specific antibody incubated in TTBS buffer (20 mM Tris-HCl pH 8.0, 500 mM NaCl and 0.05% Tween 20), followed by incubation with a secondary antibody in the same buffer. Finally, the membrane was immunochemically stained as described above for Western blot analyses [34].

2.10. Protein-protein interactions assayed by affinity chromatography

These experiments were carried out as described [20] with some modifications. The whole procedure is carried out at 4°C unless otherwise stated. The corresponding purified recombinant proteins Asa1-6H-OSCP and Asa1-OSCPΔC-6H (2 mg of each protein) were dialyzed together against PBS buffer containing 500 mM NaCl, 2% glycerol and 0.05% Tween 20, pH 7.8. The aggregated material was removed by centrifugation at 17,000 *g* for 10 min. 30 µL of equilibrated Ni Sepharose 6 FF resin (Amersham Biosciences) were added to the sample and imidazole was added to a final concentration of 30 mM from a 1 M stock solution. The sample was incubated with mild shaking for 5 hours. The resin was recovered by centrifugation at 500 *g* for 5 min and then washed 10 times with PBS buffer containing 50 mM imidazole. The washed resin was poured into a column and the proteins were eluted with a step imidazole gradient from 50 mM to 500 mM. Fractions recovered from the column were analyzed by Tricine-SDS-PAGE.

2.11 Protein structure prediction

The regions responsible for the interaction of subunits *b* and OSCP had been previously determined by X-ray diffraction: “the structure of the membrane extrinsic region of bovine ATP synthase” (PDB ID: 2WSS) [35]. The

corresponding regions of subunits *b* and OSCP were aligned with the sequences of subunits Asa1 and OSCP of *Polytomella* sp., respectively. The conserved residues between each pair of subunits were determined. The three dimensional structure of subunit OSCP of *Polytomella* sp. was modelled based on the OSCP subunit of the bovine enzyme (PDB: 2WSS) using the server Swiss Prot. In the subunit Asa1 sequence the residues adjacent to those conserved were mutated *in silico* with the software Coot (http://www2.mrc-lmb.cam.ac.uk/personal/pemsley/coot/) using the bovine model as a template. The function "regularize zone" was applied to the mutated region in order to minimize energy. The resulting models were visualized with Pymol (https://www.pymol.org/).

3. Results

3.1. Over-expression and purification of recombinant Asa subunits.

Our study focused on the interactions of subunits Asa1 and OSCP of the ATP synthase of *Polytomella* sp. using recombinant subunits. For this purpose, the proteins of interest were over-expressed and purified. Figure 1 shows a Tricine-SDS-gel with the purified recombinant subunits Asa1, OSCP with and without a histidine tag (OSCP and $OSCP_{6H}$ respectively) and a recombinant fragment of OSCP comprising residues 5-126 of the mature protein and therefore lacking the carboxy-terminal region (hereby named OSCP-Δc).

3.2. On the interaction of Asa1 and OSCP.

One strategy used to detect protein-protein interactions is Far-Western blotting. We assayed possible interactions of the purified, recombinant Asa1 subunit with the entire ATP synthase, searching for binding of the externally-added, recombinant polypeptide to some of the subunits of the complex. The ATP synthase was resolved by SDS-PAGE and transferred to nitrocellulose membranes. The strips, containing the same concentration of enzyme, were incubated with increasing concentrations of the recombinant Asa1 subunit and afterwards decorated with an anti-Asa1 antibody and the appropriate secondary

antibody (Fig 2A). The position of each of the ATP synthase subunits in the blots were identified beforehand by Ponceau S red staining.

In all lanes, as expected, the anti-Asa1 antibody recognized the Asa1 subunit of the ATP synthase, but at increasing concentrations of the externally added, recombinant Asa1, additional bands appeared on the blot, one of 31 kDa corresponding to either subunit Asa4 or gamma and one of 23 kDa corresponding to either OSCP or subunit *a* (Atp6) (Fig 2A, lanes 3 to 6). This indicated that the recombinant Asa1 subunit, incubated in a soluble form over the nitrocellulose membrane, interacted with some polypeptides of the nitrocellulose membrane-bound ATP synthase. Nevertheless, with this approach, it was impossible to distinguish if the 31 kDa band was Asa4 or gamma, since both polypeptides migrate together in the SDS-PAGE system used. The same happened with the 23 kDa band, which could correspond either to OSCP or to subunit *a* (Atp6), two polypeptides that exhibit the same mobility in our electrophoretic conditions. At higher concentrations of the externally-added, recombinant Asa1 subunit, additional faint bands were observed, that were interpreted to result from unspecific binding.

A variation of the above described experiment was carried out, in which the isolated, recombinant OSCP subunit was resolved by SDS-PAGE and transferred to nitrocellulose membranes. The strips, containing the same concentration of OSCP, were incubated with increasing concentrations of the recombinant Asa1 subunit and afterwards incubated with an anti-Asa1 antibody and the appropriate secondary antibody (Fig 2B). At increasing concentrations of the externally-added recombinant Asa1, the anti-Asa1 antibody recognized the OSCP subunit bound to the nitrocellulose membrane (Fig 2B, lanes 3 to 6). This further suggested the interaction of Asa1 and OSCP.

We previously reported a combined gel electrophoresis system that allowed almost complete resolution of all the polypeptide components of the algal ATP synthase [14]. In this 2D system, subunit OSCP was resolved from subunit *a,* and subunit Asa4 was separated from the gamma subunit. The recombinant Asa1 polypeptide was incubated with nitrocellulose membranes in which all the

subunits of the algal ATP synthase were resolved in a two dimensional array (Fig 3A). As in the 1D Far Western blot experiments, the anti-Asa1 antibody recognized only the Asa1 subunit both in the 2D array and in the control lane in which the ATP synthase was loaded as a molecular mass standard (Fig 3B). In contrast, when the 2D array blot was pre-incubated with the isolated Asa1 recombinant protein, two additional main bands were observed, that correspond to the gamma subunit and OSCP (Fig 3C). When a similar 2D-array (Fig 4A) was blotted and incubated with an anti-OSCP antibody, the OSCP subunit was clearly identified (Fig 4B). Finally, when this 2D array blot was pre-incubated with the isolated OSCP recombinant protein, three additional bands were observed, that were identified as Asa1, alpha subunit and the gamma subunit (Fig 4C). Thus, 2D-Far-Western analysis allowed us to resolve the ambiguities encountered in 1D-Far-Westerns and suggested the interactions Asa1-OSCP and Asa1-gamma.

An additional Far-Western assay was carried out in which three forms of OSCP were resolved and transferred to a nitrocellulose membrane: the recombinant protein (OSCP), the recombinant protein containing a hexa-histidine tag ($OSCP_{6H}$), and the amino-terminal fragment of the protein (OSCP-Δc). Complex V and the recombinant Asa1 protein were also transferred to the membrane (Fig 5, lanes 1-5). As in previous Far-Western blot experiments, the anti-Asa1 antibody, in the absence of externally-added Asa1 protein, recognized only the Asa1 subunit in complex V and the isolated Asa1 recombinant protein (Fig 5, lanes 6-10). By contrast, when the membrane was incubated with the Asa1 protein before the addition of the anti-Asa1 antibody, additional bands appeared in the blot: gamma and OSCP in complex V (Fig 5, lane 11), and the two forms of the intact OSCP protein ($OSCP_{6H}$ and OSCP, Fig 5, lanes 13 and 14 respectively). No antibody was bound to the fragmented OSCP subunit (OSCP-Δc, lane 15 in Fig. 5), suggesting that the carboxy-terminus of OSCP is instrumental for binding the externally added, recombinant Asa1 subunit. This experiment also suggested that the binding of Asa1 to OSCP is not spurious, since no binding of Asa1 to OSCP-Δc was observed, even when the latter was loaded at similar protein concentrations similar to OSCP.

To further explore the interaction of Asa1 and OSCP using a different experimental approach, the isolated, recombinant Asa1 protein containing a 6His-tag ($Asa1_{6H}$), was bound to a Ni Sepharose resin. Then, the recombinant OSCP (lacking a 6His-tag) was added and the resin was washed with 30 mM imidazole. In order to discard the possibility of an adventitious binding of OSCP to the nickel matrix, a second experiment was performed in which no protein was bound to the resin, but a non-tagged OSCP recombinant protein was added in parallel. While OSCP eluted in the first fractions of the column lacking bound Asa1 (Fig 6A, upper panel), a fraction of OSCP was retained in the column that contained $Asa1_{6H}$. When a 30 to 500 mM imidazole gradient was applied to the column, both OSCP and $Asa1_{6H}$ were found to elute together in several fractions (Fig 6A, lower panel). This suggested that Asa1, when bound to the nickel column, is able to bind and retain OSCP. A complementary experiment was carried out. In this case, the isolated, recombinant OSCP-Δc fragment containing a 6His-tag (OSCP-Δc_{6H}), was bound to the nickel resin. Then, the recombinant Asa1 subunit (lacking a 6His-tag) was loaded on the column and washed with 30 mM imidazole. As a control, the same nickel matrix, with no bound protein to it, was also loaded with a non-tagged Asa1 recombinant subunit and run in parallel. Asa1 eluted in the first fractions, both from the resin that lacked (Fig 6B, upper panel) and the one that contained bound OSCP-Δc_{6H} fragment (Fig 6B, lower panel). When the column was eluted with a 30 to 500 mM imidazole gradient, only the OSCP-Δc_{6H} fragment was recovered (Fig 6, lower panel). These results reinforced the idea that Asa1 does not bind to the OSCP-Δc_{6H} fragment and that therefore the carboxy-terminus of OSCP is required for Asa1 binding.

3.3. Subunit Asa1 is also found in a subcomplex containing membrane-embedded subunits.

In previous work [9], the algal ATP synthase was dissociated at relatively high temperatures. When the enzyme was heated for 30-40 sec at 60 °C a transient subcomplex of 200 kDa formed by subunits Asa1/Asa3/Asa5/Asa8/*a*/*c* was identified by first dimension Blue Native Electrophoresis followed by 2D-SDS-

PAGE; at longer time of heat treatment, this subcomplex further dissociated, giving rise to free individual subunits. Here, we looked for conditions in which a stable subcomplex containing Asa1 could be formed without heat treatment. For this purpose, the purified enzyme was incubated at 4°C overnight with increasing concentrations of lauryl maltoside. As judged by Blue Native Electrophoresis, in the presence of high detergent concentrations the dimeric complex (V_2) dissociated into its monomeric form (V) and released some free F_1 sector. A band, with a slightly faster migration than the F_1 sector was identified as a subcomplex (SC) (Fig 7A). A sample of the purified enzyme was incubated with 2.0 % lauryl maltoside overnight and was further resolved in 2D-SDS-PAGE, where the polypeptides forming this subcomplex were separated (Fig 7B). Their identities were assigned by their apparent molecular masses as Asa1 (60.6 kDa), Asa3 (36.3 kDa), Asa5 (14.3 kDa) and Asa8 (10.0 kDa). Again, the band of 23 kDa could be either subunit *a* (Atp6) or OSCP. An additional band of around 46 kDa, exhibiting mobility slightly lower than Asa2, was named tentatively AsaX. The polypeptides Asa1 and Asa8 identities were assigned immunochemically by Western blot analysis using specific antibodies (Fig 7C). Mass spectrometry analysis unambiguously revealed that the 23 kDa was subunit *a* (Atp6, GenBank: CBK55668.1) since two polypeptides of this subunit were identified: TGSLPTNFLTGVYR and SQNPAEKPHPVNDRLLPAVVDASDKR. Mass spectrometry analysis did not revealed the nature of Asax, since only minute amounts of human keratin, type II cytoskeletal keratin (NCBI Reference Sequence: NP_006112.3) were found in the sample. The band AsaX was therefore subjected to Edman degradation, revealing the N-terminal sequence S-V-L-A-A-S-K-M-V-G-A-G-X-A-T, which matches the N-terminus sequence (SVLAASKMVGAGCAT) of subunit *c* (Atp8) of *Polytomella* sp. (GenBank: ADE92942.1). Thus, AsaX seems to be a SDS-resistant oligomer of *c* subunits migrating with an apparent molecular mass of 46 kDa in SDS-PAGE. Most probably, subunit *c* escaped mass spectrometry detection due to its highly hydrophobic nature. The obtained subcomplex ASA1/ASA3/ASA5/ASA8/a/c_x seems to be identical to the one previously observed after heating for a short time

the enzyme, except that subunit *c* is now found as an oligomer forming a SDS-resistant ring, probably a decamer of *c*-subunits, as deduced from the electron cryomicroscopy map of the algal ATP synthase [16]. Asa1 is therefore associated with the membrane-bound subunits *a* (Atp6), *c* (Atp9) and Asa8, and also with the extrinsic subunits Asa5 and Asa3. Since Asa1 lacks any predictable transmembrane stretch, and therefore cannot be considered to be imbedded in the lipid bilayer, the data strongly suggests that Asa1 may be the key component that bridges the region between the inner mitochondrial membrane and OSCP. The model shown in Fig 8A integrates the results presented in this work. The model proposes Asa1 spanning the peripheral arm from a region in close proximity to the membrane (interacting with subunits Asa3, Asa5, Asa8, *a* and c_{10}), up to the F_1 region of the enzyme (where it interacts with OSCP). Some of the key residues that mediate the interaction of subunit *b* with OSCP have been identified in the crystallographic structure of the beef enzyme (PDB: 2WSS)[35]. Sequence alignments allowed us to identify several of these residues in the algal Asa1 and OSCP sequences (Supplementary Figure 1). Thus, the algal subunits OSCP and the corresponding region of Asa1 were modelled *in silico* using 2WSS as template. The resulting model is shown in Figure 8B, and the residues proposed to mediate the binding of Asa1 with OSCP are highlighted.

4. Discussion

In ATP synthases, the peripheral stalks are the structures that counteract the torque generated by rotation of the central stalk during the function of the enzyme [36, 37]. While the F-type ATPases contain only one peripheral stalk [38], A-type ATPases contain two [39] and eukaryotic V-type ATPases contain three [40]. Also, the subunit structures of the prokaryotic and eukaryotic peripheral stalks are very different. In bacteria like *Escherichia coli*, the peripheral stalk contains two identical *b* subunits, each one exhibiting one transmembrane stretch. Both subunits extend as coiled-coil structures to the top of F_1 where the δ subunit (the bacterial equivalent of OSCP) resides [41, 42]. The A_1Ao-ATP synthases also exhibit coiled-coil structures formed by the heterodimeric subunits E and G [37]. The sequence of the *b* subunit of

477 the eukaryotic peripheral stalk differs starkly from the bacterial one. The yeast and
478 beef *b* subunits contain two transmembrane stretches near their N-terminal regions
479 and extend towards the top of the F_1 sector associating with subunits *d* and F6 (*h*)
480 and reaching OSCP [21, 43]. In contrast with the above mentioned peripheral stalks,
481 the ATP synthase of the colorless alga *Polytomella* sp. exhibits an extremely robust,
482 electron-dense peripheral stalk as observed in electron microscope image
483 reconstructions [16]. The Asa subunits, present only in mitochondrial ATP synthases
484 of chlorophycean algae [19] have been pin-pointed as the main constituents of this
485 peripheral stalk. We have previously studied the arrangement of Asa subunits and
486 shown that Asa2, Asa4 and Asa7 interact, and furthermore, that the interaction of
487 Asa4 with Asa7 is mediated by the C-terminal halves of both proteins [20]. Also,
488 subunits Asa2, Asa4 and Asa7 formed a subcomplex with a 1:1:1 stoichiometry that
489 could be reconstituted in vitro. This subcomplex seems to establish contacts with
490 Asa1 and with OSCP. Here, we addressed specifically the topology of Asa1, the
491 larger polypeptide (60.6 kDa) of all Asa subunits. The location of the Asa1 subunit
492 remained controversial since on one hand, it was proposed to represent the large bulk
493 observed in the top region of the peripheral stalk in close contact with the F_1 sector
494 [17] and on the other hand it was identified to constitute a subcomplex along with
495 subunits Asa3, Asa5, Asa8, *a* and *c*, and therefore it was considered to be in close
496 vicinity with the matrix-exposed surface of the inner mitochondrial membrane [9].
497 The data presented in this work suggest that Asa1 interacts strongly with the OSCP
498 subunit. Asa1 seems to be one of the main components of the peripheral stalk of the
499 algal enzyme forming a physical bridge between the extrinsic subunits (mainly
500 OSCP) and other components of the enzyme either imbedded or in close contact
501 with the membrane (Asa3, Asa5, Asa8, *a* and *c*-ring). Thus, Asa1 seems to be the
502 main support of the peripheral stalk, further reinforced by other Asa subunits (Asa2,
503 Asa4, Asa7), playing a structural role similar to the one of subunit *b* in orthodox
504 enzymes.
505 The interaction Asa1 subunit-gamma subunit, as observed in the Far Western
506 blot experiments, is hard to explain, since in order for the ATP synthase to work as a
507 nanomotor, the rotary components should not interact directly with stator

components. A tight binding of Asa1 to the gamma subunit would obviously impede its rotation. We therefore consider that the binding of Asa1 to the gamma subunit, as judged by Far-Western Blotting, to be unspecific and probably due to the propensity of both proteins to form coil-coiled structures.

The electron cryo-microscopy map of the algal ATP synthase also shows that the *c*-ring is formed by 10 monomers [16]. In this work, we observed the presence of a high molecular mass *c*-ring in SDS-PAGE. This band was not observed before in other *Polytomella* ATP synthase preparations because it co-migrates with subunit Asa2 in SDS-PAGE with an apparent molecular mass of 45.5 kDa. The band, initially named AsaX, was identified as subunit *c* by N-terminal sequencing by Edman degradation. Thus, the algal F_1Fo-ATP synthase exhibits a SDS-resistant *c*-ring similar to those previously observed in various isolated Na^+-dependent A_1Ao-ATP synthases, including the strictly anaerobic bacterium *Propionigenium modestum* [44], the fusobacterium *Ilyobacter tartaricus* [45], the acetogenic bacterium *Acetobacterium woodii* [46], and the hyperthermophilic archaea *Pyrococcus furiosus* [47] and *Thermococcus onnurineus* [48]. To our knowledge, this could be the first report of a H^+-dependent F_1Fo-ATP synthase exhibiting a SDS-resistant *c*-ring.

Analysis of the Asa subunit sequences indicated high propensity of Asa1, Asa2, Asa4 and Asa7 to form coiled-coil regions (30, 19, 35 and 32% respectively) [20]. These Asa subunits most probably interact through large contacts within alpha-helices that form the robust, intertwined peripheral arm observed in the electron cryo-microscopy map of the *Polytomella* ATP synthase dimer [16]. The size of the F_1 sector [$\alpha_3/\beta_3/\gamma/\delta/\varepsilon$] is around 150 Å, so one can estimate the length of the peripheral stalk of the *Polytomella* enzyme to be of 221 Å, taking into account the curvature observed in the electron cryo-microscopy map of the enzyme [16]. The mature Asa1 subunit has 596 residues, so if one considers the whole protein to be in an alpha-helical conformation, it should have a length of 894 Å, enough to transverse the peripheral stalk three to four times. In contrast, subunit *b* of the orthodox ATP synthases green algae, is around 190 residues (285 Å long), thus only one third of the Asa1 subunit.

In this work, we provide evidence for the interaction of Asa1 subunit that seem to pertain solely to the chlorophycean algal lineage with one of the highly conserved subunits present in all mitochondrial ATP synthases known to date (the OSCP subunit). We suggest that Asa1 has taken the place of subunit *b* as the main constituent of the mitochondrial ATP synthase peripheral arm. Genes encoding orthodox *b* subunits are found in almost all land plants and green alga. The distribution of *b* subunits and Asa1 subunits in different photosynthetic organisms is shown in Suppl. Fig. 2. While land plants, Charophyte alga, Prasinophytes, and the class Trebouxiophyceae exhibit a gene encoding orthodox subunit *b*, this gene is absent and seems to be substituted by the gene encoding Asa1 in Chlorophycean algae, both in the orders Chlamydomonadales and Sphaeropleales. The origin of Chlorophyceae occurred approximately 600 million years ago [49]. The origin of this lineage seems to be related to the drastic reduction of mitochondrial genome in size and in gene content, and to the appearance of nucleus-encoded atypical subunits of the enzyme (Asa subunits) [50, 19].The phylogenetic distribution of orthodox *b* subunits and Asa1 subunits strongly suggests that the appearance during evolution of Asa subunits as constituents of the ATP synthase peripheral arm, only occurred in Chlorophycean algae. One could predict that the OSCP subunit of Chlorophycean algae must also differ from classical plant and algal OSCP subunits, in order to accommodate binding to the Asa1 subunit instead of the *b* subunit. Alignment of diverse OSCP primary sequences strongly suggests that this protein separates into two clearly distinct groups that exhibit conspicuously different amino acid sequences: one of Chlorophycean algae and another of all the other green algae and land plants (Supplementary Fig. 3).

It seems that Asa1 is neither a highly modified subunit b nor the result of a duplication of a gene encoding subunit *b*. Rather; it seems more likely that in the chlorophycean lineage, all the orthodox structural components of the peripheral arm were substituted by scaffold-forming proteins from a complete different origin, i.e., the Asa subunits.

Acknowledgments

We thank Laura Ongay Larios, Minerva Mora Cabrera and Guadalupe Códiz Huerta of the Molecular Biology Unit, IFC, UNAM for primer synthesis and sequencing. This research was supported by the grant 245486 from the Consejo Nacional de Ciencia y Tecnología (CONACyT) and the Belgian Fonds de la Recherche Scientifique (F.R.S.-FNRS) (Mexico-Belgium). Additional support was received from grants 239219 (CONACyT, Mexico), IN203311-3 from the Dirección General de Asuntos del Personal Académico (DGAPA-UNAM, Mexico) and from the Belgian F.R.S.-FNRS (MIS F.4520, FRFC 2.4597). CONACyT also supported with fellowship 599282 the Ph.D. studies of L.C.-T. (Biomedical Sciences Ph.D. program at UNAM).

References

1] T., Xu, V., Pagadala, D.M., Mueller, Understanding structure, function, and mutations in the mitochondrial ATP synthase. Microb. Cell. 2(2015) 105-125.

2] A., Wächter, Y. Bi, S.D., Dunn, B.D., Cain, H., Sielaff, F., Wintermann, S., Engelbrecht, W., Junge, Two rotary motors in F-ATP synthase are elastically coupled by a flexible rotor and a stiff stator stalk. Proc. Natl. Acad. Sci. USA 108 (2011) 3924-3929.

3] J.E. Walker, V.K. Dickson, The peripheral stalk of the mitochondrial ATP synthase, Biochim. Biophys. Acta, 1757 (2006) 286-296.

4] H. Seelert, N.A. Dencher, ATP synthase superassemblies in animals and plants: two or more are better. Biochim Biophys Acta. 1807 (2011) 1185-1197.

5] P., Paumard, J., Vaillier, B., Coulary, J., Schaeffer, V., Soubannier, D.M., Mueller, D., Brèthes, J.P., di Rago, J., Velours, The ATP synthase is involved in generating mitochondrial cristae morphology.EMBO J. 21(2002) 221-230.

6] N.P., Balabaskaran, N.V., Dudkina, L.A. Kane, J.E. van Eyk, E.J. Boekema, M.W. Mather, A.B. Vaidya, Highly divergent mitochondrial ATP synthase complexes in *Tetrahymena thermophila*. PLoS Biol. 8 (2010) e1000418.

7] A. Zikova, A. Schnaufer, R.A. Dalley, A.K. Panigrahi, K.D. Stuart, The F(0)F(1)-ATP synthase complex contains novel subunits and is essential for procyclic *Trypanosoma brucei*. PLoS Pathog. 5 (2009) e1000436.

8] E., Perez, M., Lapaille, H., Degand, L., Cilibrasi, A., Villavicencio-Queijeiro, P., Morsomme, D., González-Halphen, M.C., Field, C., Remacle, D., Baurain, P., Cardol, The mitochondrial respiratory chain of the secondary green alga *Euglena gracilis* shares many additional subunits with parasitic Trypanosomatidae. Mitochondrion. 19 Pt B (2014) 338-349.

9] M. Vázquez-Acevedo, P. Cardol, A. Cano-Estrada, M. Lapaille, C. Remacle, D. González-Halphen, The mitochondrial ATP synthase of chlorophycean algae

contains eight subunits of unknown origin involved in the formation of an atypical stator-stalk and in the dimerization of the complex. J. Bioenerg. Biomembr. 38 (2006) 271-282.

10] R. van Lis, A. Atteia, G. Mendoza-Hernández, D. González-Halphen, Identification of novel mitochondrial protein components of Chlamydomonas reinhardtii. A proteomic approach. Plant Physiol. 132 (2003) 318-330.

11] A., Atteia, G., Dreyfus, D., González-Halphen, Characterization of the alpha and beta-subunits of the F0F1-ATPase from the alga *Polytomella* spp., a colorless relative of *Chlamydomonas reinhardtii*, Biochim. Biophys. Acta 1320 (1997) 275-284.

12] N.V. Dudkina, J. Heinemeyer, W. Keegstra, E.J. Boekema, H.P. Braun, Structure of dimeric ATP synthase from mitochondria: an angular association of monomers induces the strong curvature of the inner membrane. FEBS Lett. 579 (2005) 5769-5772.

13] N.V. Dudkina, S. Sunderhaus, H.P. Braun, E.J. Boekema, Characterization of dimeric ATP synthase and cristae membrane ultrastructure from *Saccharomyces* and *Polytomella* mitochondria. FEBS Lett. 580 (2006) 3427-3432.

14] A. Cano-Estrada, M. Vázquez-Acevedo, A. Villavicencio-Queijeiro, F. Figueroa-Martínez, H. Miranda-Astudillo, Y. Cordeiro, J.A. Mignaco, D. Foguel, P. Cardol, M. Lapaille, C. Remacle, S. Wilkens, D. González-Halphen, Subunit-subunit interactions and overall topology of the dimeric mitochondrial ATP synthase of *Polytomella* sp. Biochim Biophys Acta. 1797 (2010) 1439-1448.

15] N.V. Dudkina, G.T. Oostergetel, D. Lewejohann, H.P. Braun, E.J. Boekema, Row-like organization of ATP synthase in intact mitochondria determined by cryo-electron tomography. Biochim. Biophys. Acta. 1797 (2010) 272-277.

16] M., Allegretti, N., Klusch, D.J., Mills, J., Vonck, W. Kühlbrandt, K.M. Davies, Horizontal membrane-intrinsic α-helices in the stator a-subunit of an F-type ATP synthase, Nature 521(2015) 237-240.

17] R. van Lis, G. Mendoza-Hernández, G. Groth, A. Atteia, New insights into the unique structure of the F0F1-ATP synthase from the chlamydomonad algae *Polytomella* sp. and *Chlamydomonas reinhardtii*. Plant Physiol. 144 (2007) 1190-1199.

18] A. Villavicencio-Queijeiro, M. Vázquez-Acevedo, A. Cano-Estrada, M. Zarco-Zavala, M. Tuena de Gómez, J.A. Mignaco, M.M. Freire, H.M. Scofano, D. Foguel, P. Cardol, C. Remacle, D. González-Halphen, The fully-active and structurally-stable form of the mitochondrial ATP synthase of *Polytomella* sp. is dimeric. J. Bioenerg. Biomembr. 41 (2009) 1-13.

19] M. Lapaille, A. Escobar-Ramírez, H. Degand, D. Baurain, E. Rodríguez-Salinas, N. Coosemans, M. Boutry, D. Gonzalez-Halphen, C. Remacle, P. Cardol, Atypical subunit composition of the chlorophycean mitochondrial F1FO-ATP synthase and role of Asa7 protein in stability and oligomycin resistance of the enzyme. Mol. Biol. Evol. 27 (2010) 1630-1644.

20] H., Miranda-Astudillo, A., Cano-Estrada, M., Vázquez-Acevedo, L., Colina-Tenorio L, A., Downie-Velasco, P., Cardol, C., Remacle, Domínguez-Ramírez, L., González-Halphen D. Interactions of subunits Asa2, Asa4 and Asa7 in the peripheral stalk of the mitochondrial ATP synthase of the chlorophycean alga *Polytomella* sp. Biochim Biophys Acta. (2014) 1837: 1-13.

21] V.K., Dickson, J.A., Silvester, I.M., Fearnley, A.G., Leslie, J.E. Walker, On the structure of the stator of the mitochondrial ATP synthase. EMBO J. 25(2006) 2911-2918.

22] L.A., Baker, I.N., Watt, M.J., Runswick, J.E., Walker, J.L., Rubinstein, Arrangement of subunits in intact mammalian mitochondrial ATP synthase determined by cryo-EM. Proc. Natl. Acad. Sci. USA, 109(2012) 11675-11680.

23] W.C., Lau, L.A., Baker, J.L. Rubinstein, Cryo-EM structure of the yeast ATP synthase, J. Mol. Biol. 382(2008):1256-1264.

24] C., Mellwig, B., Böttcher A unique resting position of the ATP-synthase from chloroplasts. J Biol Chem. 278(2003) 18544-18549.

25] I., Ogilvie, S., Wilkens, A.J., Rodgers, R., Aggeler, R.A., Capaldi. The second stalk: the delta-b subunit connection in ECF1F0. Acta Physiol. Scand. Suppl. 643 (1988) 169-175.

26] H. Schägger, Denaturing Electrophoretic Techniques, in G. von Jagow, H. Schägger (Eds), A Practical Guide to Membrane Protein Purification, Academic Press, San Diego, (1994a) pp. 59-79.

27] U.K., Laemmli, Cleavage of structural proteins during the assembly of the head of bacteriophage T4, Nature 227 (1970) 680-685.

28] H. Schägger, Native Gel Electrophoresis, in G. von Jagow, H. Schägger (Eds), A Practical Guide to Membrane Protein Purification, Academic Press, San Diego, (1994b), pp. 81-104.

29] M.A.K., Markwell, S.M., Hass, L.L., Biber, N.E., Tolbert, A modification of the Lowry procedure to simplify protein determination in membrane and lipoprotein samples. Anal. Biochem. 87 (1978) 206-210.

30] A., Atteia, R.,van Lis, S.I., Beale, Enzymes of the heme biosynthetic pathway in the nonphotosynthetic alga *Polytomella* sp., Eukaryot. Cell 4 (2005) 2087-2097.

31] H. Schägger, H. Aquila, G. Von Jagow, Coomassie blue-sodium dodecyl sulfate-polyacrylamide gel electrophoresis for direct visualization of polypeptides during electrophoresis. Anal. Biochem. 173 (1988) 201-205.

32] D. González-Halphen, M.A. Lindorfer, R.A. Capaldi, Subunit arrangement in beef heart complex III. Biochemistry 27 (1988) 7021-7031.

33] R. A., Hall, Studying protein-protein interactions via blot overlay or Far Western blot, Methods in Molecular Biology 261 (2004) 167-174.

34] H. Towbin, T. Staehelin, J. Gordon, Electrophoretic transfer of proteins from polyacrylamide gels to nitrocellulose sheets: procedure and some applications. Proc. Natl. Acad. Sci. U S A. 76 (1979) 4350-4354.

35] D.M. Rees, A.G. Leslie, J.E. Walker, The structure of the membrane extrinsic region of bovine ATP synthase. Proc. Natl. Acad. Sci. U.S.A. 106 (2009) 21597–21601.

36] W. Junge, H. Sielaff, S. Engelbrecht, Torque generation and elastic power transmission in the rotary F(O)F(1)-ATPase. Nature 459 (2009) 364-370.

37] A.G., Stewart, L.K., Lee, M., Donohoe, J.J., Chaston, D., Stock, The dynamic stator stalk of rotary ATPases. Nat Commun. 3 (2012) 687.

38] S., Wilkens, R.A., Capaldi, ATP synthase's second stalk comes into focus. Nature 393 (1998) 29.

39] J., Vonck, K.Y., Pisa, N., Morgner, B., Brutschy, V., Muller, Three-dimensional structure of A_1A0 ATP synthase from the hyperthermophilic archaeon *Pyrococcus furiosus* by electron microscopy. J. Biol. Chem. 284 (2009) 10110–10119.

40] Z., Zhang, Y., Zheng, H., Mazon, E., Milgrom, N., Kitagawa, E., Kish-Trier, A.J., Heck, P.M., Kane, S., Wilkens, Structure of the yeast vacuolar ATPase. J. Biol. Chem. 283 (2008) 35983-35995.

41] K.S., Wood, S.D., Dunn, Role of the asymmetry of the homodimeric b_2 stator stalk in the interaction with the F1 sector of *Escherichia coli* ATP synthase. J Biol Chem. 282(2007) 31920-31927.

42] K., Brandt, S.,Maiwald, B., Herkenhoff-Hesselmann, K.,Gnirß, J.C., Greie, S.D., Dunn, G., Deckers-Hebestreit G., Individual interactions of the b subunits within the stator of the Escherichia coli ATP synthase. J Biol Chem. 288(2013) 24465-24479.

43] M.F., Paul, B., Guerin, J., Velours, The C-terminal region of subunit 4 (subunit b) is essential for assembly of the F0 portion of yeast mitochondrial ATP synthase. Eur J Biochem. 205(1992) 163-72.

44] W., Laubinger, P., Dimroth, Characterization of the ATP synthase of Propionigenium modestum as a primary sodium pump. Biochemistry, 27 (1988) 7531-7537.

45] H., Stahlberg, D.J., Müller, K., Suda, D., Fotiadis, A., Engel, T., Meier, U., Matthey, P. Dimroth, Bacterial Na(+)-ATP synthase has an undecameric rotor. EMBO Rep. 2 (2001) 229-233.

46] M., Fritz, V., Müller V, An intermediate step in the evolution of ATPases--the F1F0-ATPase from *Acetobacterium woodii* contains F-type and V-type rotor subunits and is capable of ATP synthesis. FEBS J. 274(2007) 3421-3428.

47] K.Y., Pisa, H., Huber, M. Thomm, V., Müller, A sodium ion-dependent A_1AO ATP synthase from the hyperthermophilic archaeon *Pyrococcus furiosus*, FEBS J. 274(2007) 3928-3938.

48] F., Mayer, J.K., Lim, J.D., Langer, S.G., Kang, V., Müller, Na+ transport by the A1AO-ATP synthase purified from *Thermococcus onnurineus* and reconstituted into liposomes, J Biol Chem. 290(2015) 6994-7002.

49] M.D., Herron, J.D., Hackett, F.O. Aylward, R.E., Michod, Triassic origin and early radiation of multicellular volvocine algae. Proc. Natl. Acad. Sci. USA 106(2009) 3254-3258.

50] P., Cardol, D., González-Halphen, A., Reyes-Prieto, D., Baurain, R.F., Matagne, C., Remacle, The mitochondrial oxidative phosphorylation proteome of *Chlamydomonas reinhardtii* deduced from the Genome Sequencing Project. Plant Physiol. 137(2005) 447-459.

51] L.A., Lewis, R.M., McCourt, Green algae and the origin of land plants, Am. J. Bot. 91 (2004) 1535-1556.

52] F., Leliaert, D.R., Smith, H., Moreau, M.D., Herron, H., Verbruggen, C.F., Delwiche, O., De Clerck, Phylogeny and molecular evolution of the green algae Critical Reviews in Plant Sciences 31 (2012) 1-46.

FIGURE LEGENDS

FIGURE 1. *Polytomella* ATP synthase and the recombinant subunits used in this work.

Tricine-SDS polyacrylamide gel showing the identity of the 16 subunits of the *Polytomella* ATP synthase complex (25 µg of protein, lane 1). Three µg of each overexpressed and purified recombinant subunit were loaded in lanes 2 to 5. Molecular masses were calculated using as molecular mass marker the well-characterized polypeptide composition of the algal ATP synthase (lane 1), 62.3 kDa for Asa1 (lane 2), 22.9 kDa for OSCP-6H (lane 3), 20.3 kDa for OSCP (lane 4), and 15.4 kDa for OSCP-Δc (lane 5).

FIGURE 2. Interaction of Asa1 with polypeptides of the algal ATP synthase and the OSCP subunit.

Far-western analysis of *Polytomella* ATP synthase (25 µg of protein per lane) (panel A) and of the purified, recombinant OSCP polypeptide (panel B) incubated for 4 hours with increasing quantities of the isolated, recombinant Asa1 polypeptide as indicated (total nanomoles of Asa1 in a 5 mL final volume), and then decorated with an anti-Asa1 antibody. The identity of the main bands are indicated.

FIGURE 3. Interaction of Asa1 with the gamma and OSCP subunits.

A) 2D resolution of the polypeptides that constitute the mitochondrial *Polytomella* F_1Fo-ATP synthase. Polytomella ATP synthase (100 µg of protein) was resolved in a glycine–SDS–PAGE system (10% acrylamide). The 1D gel was then subjected to 2D tricine–SDS–PAGE (14% acrylamide) and stained with Coomassie brilliant blue. A lane loaded with the enzyme on the left-hand side of the 2D gel indicates the subunits of interest. B) Western blot analysis of the *Polytomella* ATP synthase resolved by 2D tricine–SDS–PAGE. A gel equivalent to the one shown in panel A was transferred to a nitrocellulose membrane and decorated with an anti-Asa1 antibody. C) Far-western blot analysis of the *Polytomella* ATP synthase resolved by 2D tricine–SDS–PAGE. A gel equivalent to the one shown in panel A was transferred to a nitrocellulose membrane and incubated for 4 hours with 2.0 nanomoles of the isolated, recombinant Asa1 protein, and then decorated with an anti-Asa1 antibody.

FIGURE 4. Interaction of OSCP with subunits of the algal ATP synthase. A) 2D resolution of the algal F_1Fo-ATP synthase. Polytomella ATP synthase (100 µg of protein) was resolved in 1D in a glycine–SDS–PAGE system (10% acrylamide) and then in 2D in a tricine–SDS–PAGE (14% acrylamide) and stained with Coomassie brilliant blue. The subunits of interest are indicated on the polypeptide pattern of the enzyme loaded on the left-hand side of the 2D gel. B) Western blot analysis of the *Polytomella* ATP synthase resolved by 2D tricine–SDS–PAGE. A gel equivalent to the one shown in panel A was transferred to a nitrocellulose membrane and decorated with an anti-OSCP antibody. C) Far-western blot analysis of the *Polytomella* ATP synthase resolved by 2D tricine–SDS–PAGE. A gel equivalent to the one shown in panel A was transferred to a nitrocellulose membrane and incubated for 4 hours with 2.0 nanomoles of the isolated, recombinant OSCP protein, and then decorated with an anti-OSCP antibody.

FIGURE 5. The carboxy-terminus region of OSCP is instrumental for its interaction with Asa1

A) Coomassie Blue-stained Tricine-SDS polyacrylamide gel showing the *Polytomella* ATP synthase complex (25 µg of protein, lane 1) and three µg of each of the following overexpressed and purified recombinant proteins: Asa1 (lane 2); OSCP-6H (lane 3); OSCP (lane 4) and OSCP-Δc (lane 5). [This gel is the same one shown in Figure 1]. B) Western blot analysis of an equivalent gel as the one shown in panel A. After transfer to a nitrocellulose membrane, the blot was decorated with an anti-Asa1 antibody. C) Far-western blot analysis of an equivalent gel as the one shown in panel A. After transfer to a nitrocellulose membrane, the blot was incubated for 4 hours with 2.0 nanomoles of the isolated, recombinant Asa1 protein, and then decorated with an anti-Asa1 antibody.

FIGURE 6. The interaction of Asa1 with OSCP assayed by affinity chromatography.

A) Interaction of Asa1 and OSCP assayed by affinity chromatography. The purified, recombinant OSCP subunit was bound to a Ni Sepharose resin containing no bound protein (upper panel) or to which Asa1, containing a 6His-tag, was bound (lower panel). Coomassie stained gels of the column fractions collected upon application of a 30-500 mM imidazole gradient. Lane 1, added sample; lane 2, protein excluded from the resin; lanes 3 and 4, proteins excluded after washing with 30 mM imidazole. B) Interaction of Asa1 and OSCP-Δc assayed by affinity chromatography. The experiment was carried out as described for panel A, except that the purified, recombinant OSCP-Δc fragment, lacking the carboxy-terminus of the OSCP subunit was used. The crossed arrow denotes no association between Asa1 and OSCP-Δc.

FIGURE 7. Formation and characterization of an ASA1/ASA3/ASA5/ASA8/a/c subcomplex.

A) BN-PAGE of purified ATP synthase samples incubated overnight at 4 °C under mild agitation in the presence of lauryl-maltoside at the indicated increasing concentrations (% w/v). 100 μg of protein were loaded in each lane. The control lane in the absence of the detergent is labelled 0. Dimer (V2), monomer (V); F1 sector (F1), and subcomplex (SC) are indicated. B) 2D gel of an ATP synthase sample incubated overnight in the presence of 2.0 % lauryl-maltoside. Six polypeptide bands were resolved for the subcomplex (SC) in the 2D-SDS-Tricine gel. C) Immunochemical identification of subunits Asa1 and Asa8 as constituents of the subcomplex.

FIGURE 8. Models for the interaction Asa1-OSCP.

A) Fig. 7. Subunit arrangement of the algal dimeric mitochondrial ATP synthase. The disposition of Asa1 and OSCP subunits is highlighted. Only half of the dimer is shown. B) Model for the interaction Asa1 and the carboxy-terminal region of OSCP. The algal OSCP subunit and a region of the algal Asa1subunit were modelled on the crystallographic structure of the bovine enzyme (PDB: 2WSS) [35]. The N-terminal section of OSCP is shown in fuchsia and the C-terminus in

cyan. The region of Asa1 modeled upon the 3-D structure of subunit *b* is shown in green. The residues found in the beef heart subunits *b* and OSCP that are also present in the algal subunits Asa1 and OSCP are depicted in black and are those marked on the alignment shown in Supplementary Figure 1.

Supplementary Material

Figure S1. Conserved motifs in the algal Asa1 and OSCP subunits may mediate their interaction. Some of the key residues that mediate the interaction of subunit *b* and OSCP found in the bovine crystallographic structure (PDB: 2WSS) [35] were also identified in the algal Asa1 and OSCP subunits by sequence alignments. The conserved residues in the algal sequences that are proposed to make contacts between the two subunits are shown in blue for OSCP and in green for Asa1.

Figure S2. **Phylogenetic relationships in the green lineage (Archaeplastida): distribution of genes encoding subunit *b* and subunit Asa1.**
The figure illustrates the phylogenetic relationships between organisms pertaining to the green lineage, showing in greater detail the lineages of Chlorophycean algae (adapted from [51] and [52]). The black region of the tree indicates presence of genes encoding orthodox subunit *b*, the red region indicates the presence of genes encoding Asa1 and other Asa subunits. The appearance of Asa1 subunits may have happened either in the circle indicating number 1 or in the one indicating number 2. Sequences of genes encoding the orthodox subunit *b* were found in Embriophytes: *Arabidopsis thaliana* (NCBI: NP_085524) and many other land plants; Charophyte algae: *Chara vulgaris* (NCBI: NP_943702), *Microspora stagnorum* (NCBI: YP_008816106) and *Nitella hyaline* (NCBI: YP_006073038; in Prasinophytes: *Bathycoccus prasinos* (NCBI: YP_008994804), *Monomastix* sp. (NCBI: YP_008802543), *Micromonas pusilla* (NCBI: ACO50726), *Micromonas* sp. (NCBI: YP_002860120) and *Ostreococcus tauri* (NCBI: YP_717287); and Class Trebouxiophyceae: *Auxenochlorella protothecoides* (NCBI: YP_009112927),

Chlorella sorokiniana (NCBI: YP_009049995), *Chlorella* sp. ArM0029B (NCBI: AGZ19403), *Chlorella variabilis* (NCBI: YP_009094937), *Coccomyxa subellipsoidea* C-169 (NCBI: YP_004339028), *Helicosporidium* sp. (NCBI: YP_006280974), *Lobosphaera incisa* (NCBI: YP_009138087), *Trebouxia aggregata* (NCBI: ABX82555), *Trebouxiophyceae* sp. (NCBI: YP_006666412), and *Prototheca wickerhamii* (NCBI: NP_042255). No data is available for Ulvophyceae. In stark contrast, the gene encoding subunit *b* is absent and seems to be substituted by the gene encoding Asa1 only in Chlorophycean algae, both in Chlamydomonadales like *Dunaliella tertiolecta* (iMicrobe: CCMP1320), *Chlamydomonas chlamydogama* (iMicrobe: MMETSP1392), *Chlamydomonas leiostraca* (iMicrobe: MMETSP1391), *Chlamydomonas reinhardtii* (NCBI: XP_001692395), *Chlamydomonas* sp. (iMicrobe: MMETSP1180), *Polytomella* sp. (NCBI: CAD90158), *Volvox carteri* (NCBI: XP_002951807), and in a single representative of Sphaeropleales: *Monoraphidium neglectum* (NCBI: KIZ00175). No data is currently available for Oedogoniales, Chaetophorales or Chaetopeptidales.

Figure S3. Alignment of OSCP sequences from different photosynthetic organisms. Conserved residues found in all sequences are shaded in gray. OSCP sequences group in two blocks with distinct amino acid sequences: the Chlorophycean algae (conserved residues shaded in yellow) and the rest of photosynthetic organisms (conserved residues shaded in cyan). Sequences used in this analysis were obtained from TaxoBlast (https://giavap-genomes.ibpc.fr/cgi-bin/AlgoBLAST/algoBlast_mainpage.php) or NCBI: *Auxenochlorella protothecoides* (Trebouxiophyceae), *Klebsormidium flaccidum* (Charophyte), *Coccomyxa subellipsoidea* (Trebouxiophyceae), *Chlorokybus atmophyticus* (Charophyte), *Arabidopsis thaliana* (Embriophyte), *Penium margaritacium* (Charophyte), *Pyramimonas obovate* (Prasinophyte), *Pyramimonas amylifera* (Prasinophyte), *Ostreococcus lucimarinus* (Prasinophyte), *Prasinococcus capsulatus* (Prasinophyte), and the following Chlorophyceae: *Polytomella parva*, *Chlamydomonas reinhardtii*, *Volvox carteri*, *Chlamydomonas chlamydogama*,

956 *Chlamydomonas euryale*, *Chlamydomonas leiostraca*, *Chlamydomonas* sp
957 CCMP681 and *Dunaliella tertiolecta*.

Figure 01

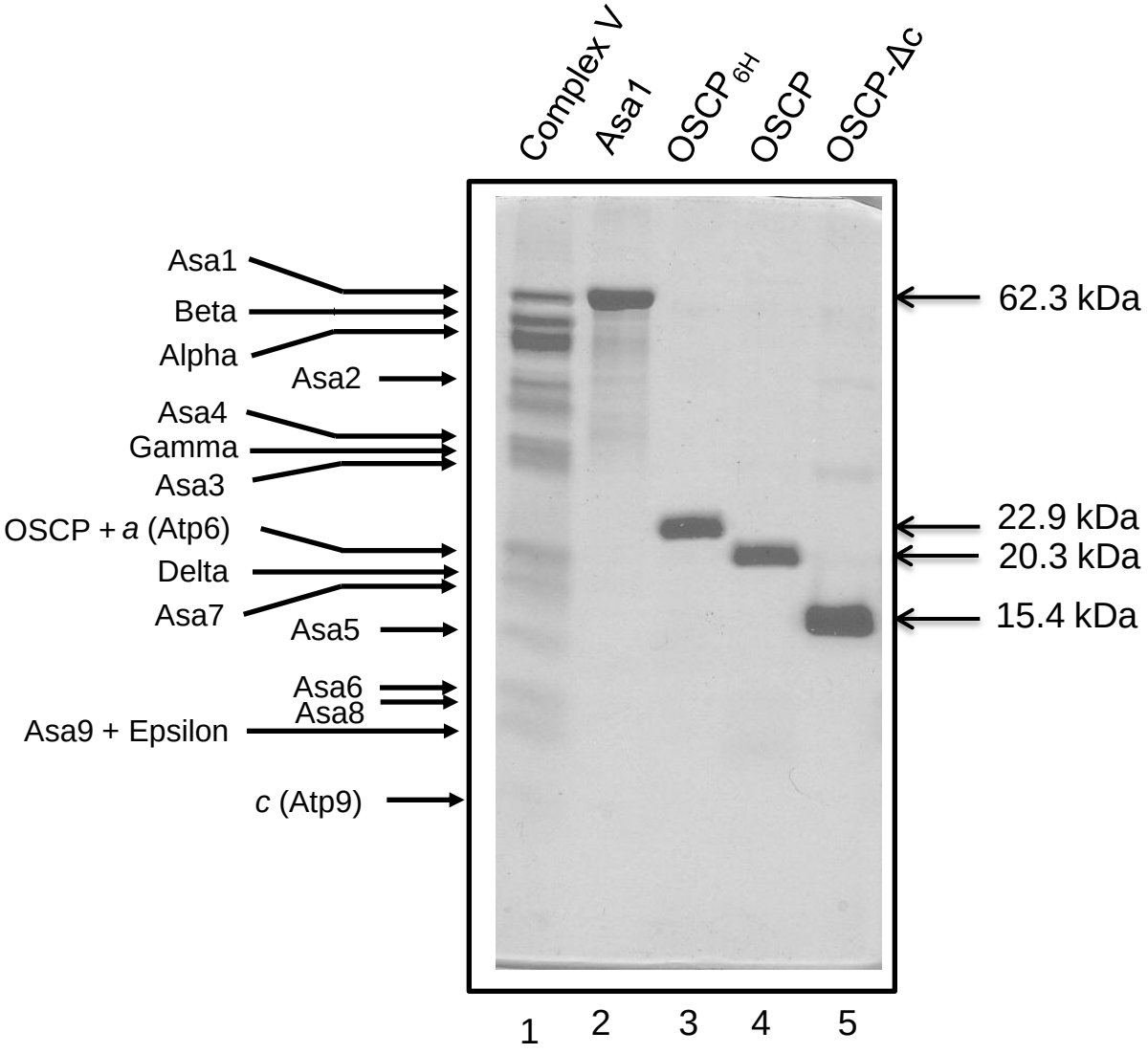

Figure 1

Figure 02A

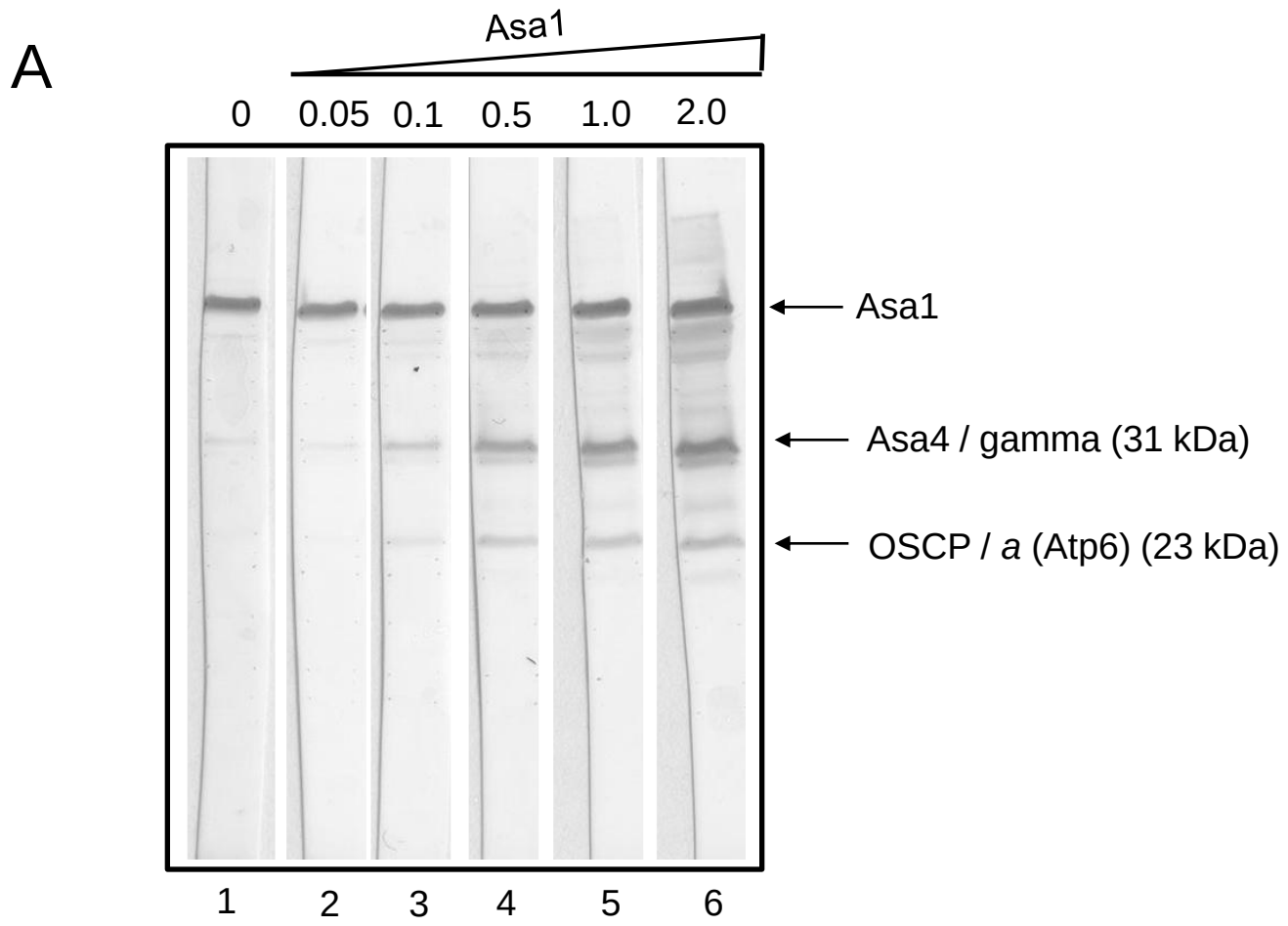

Figure 2

Figure 02B

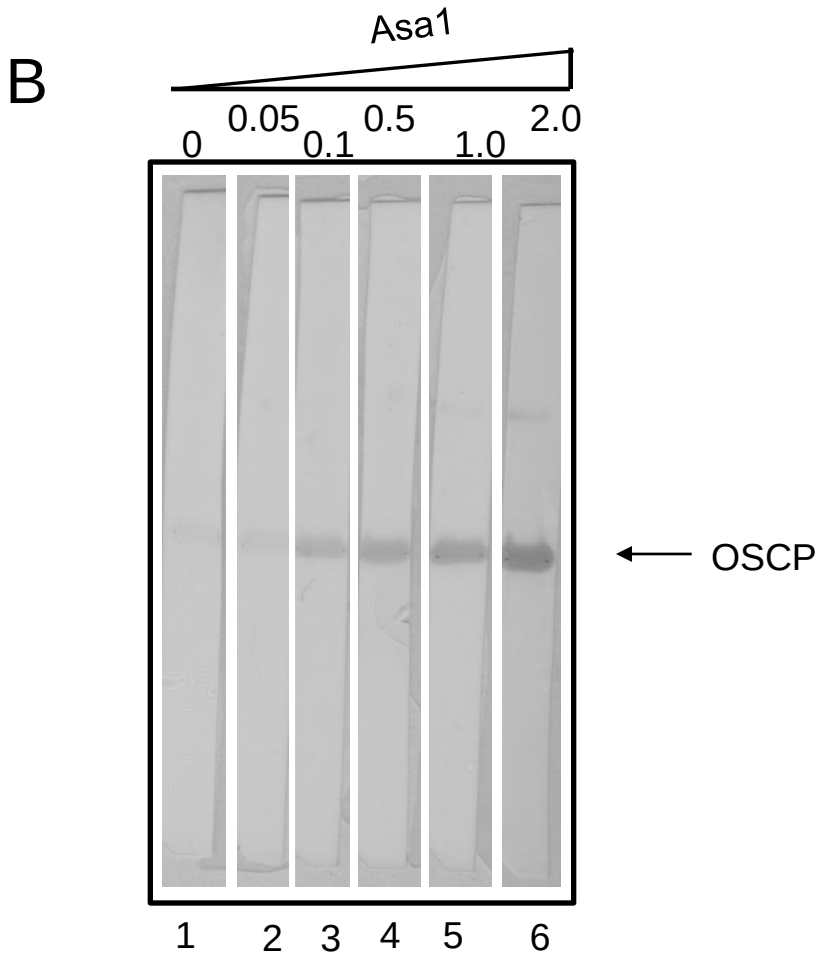

Figure 2 (continued)

Figure 03

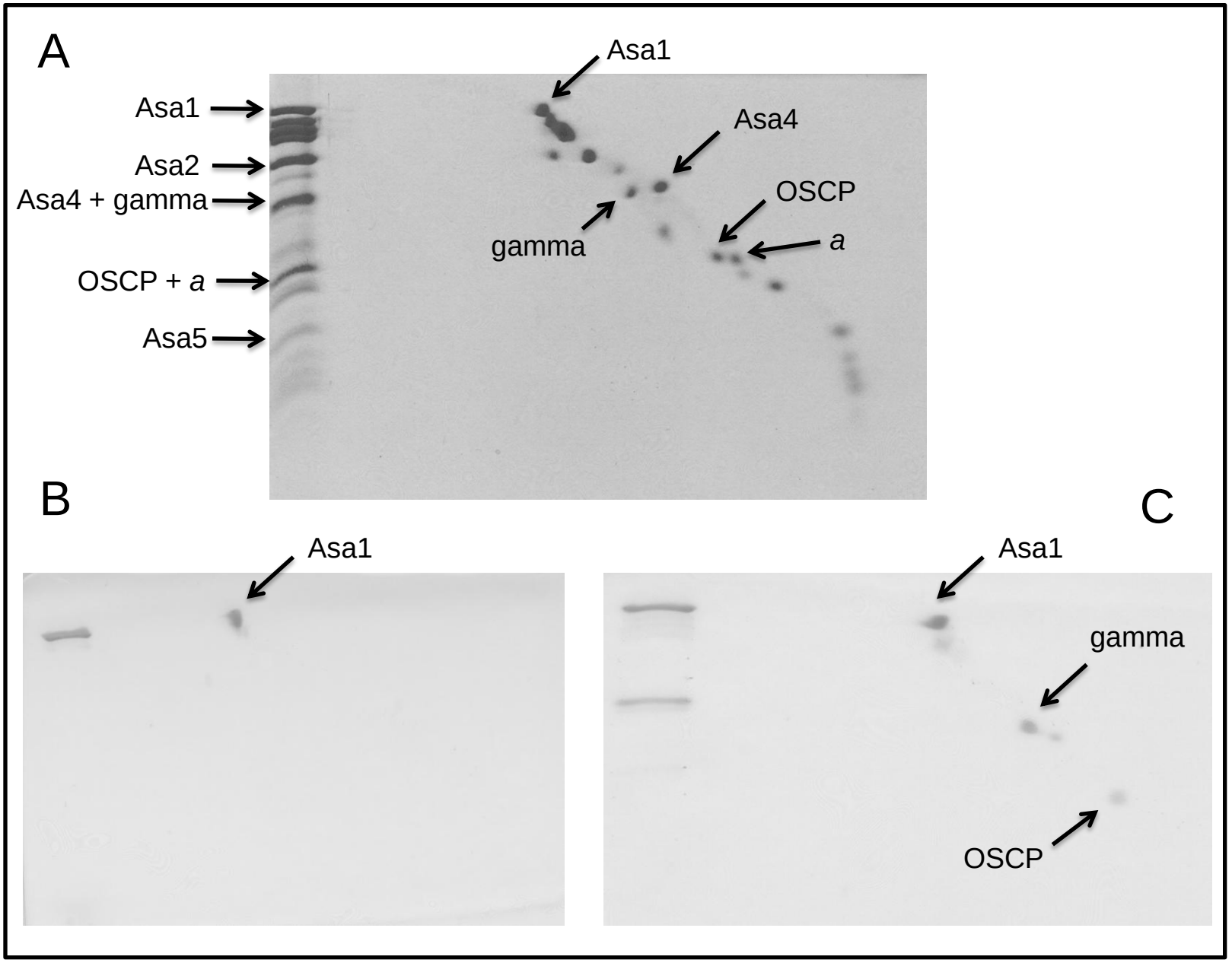

Figure 3

Figure 04

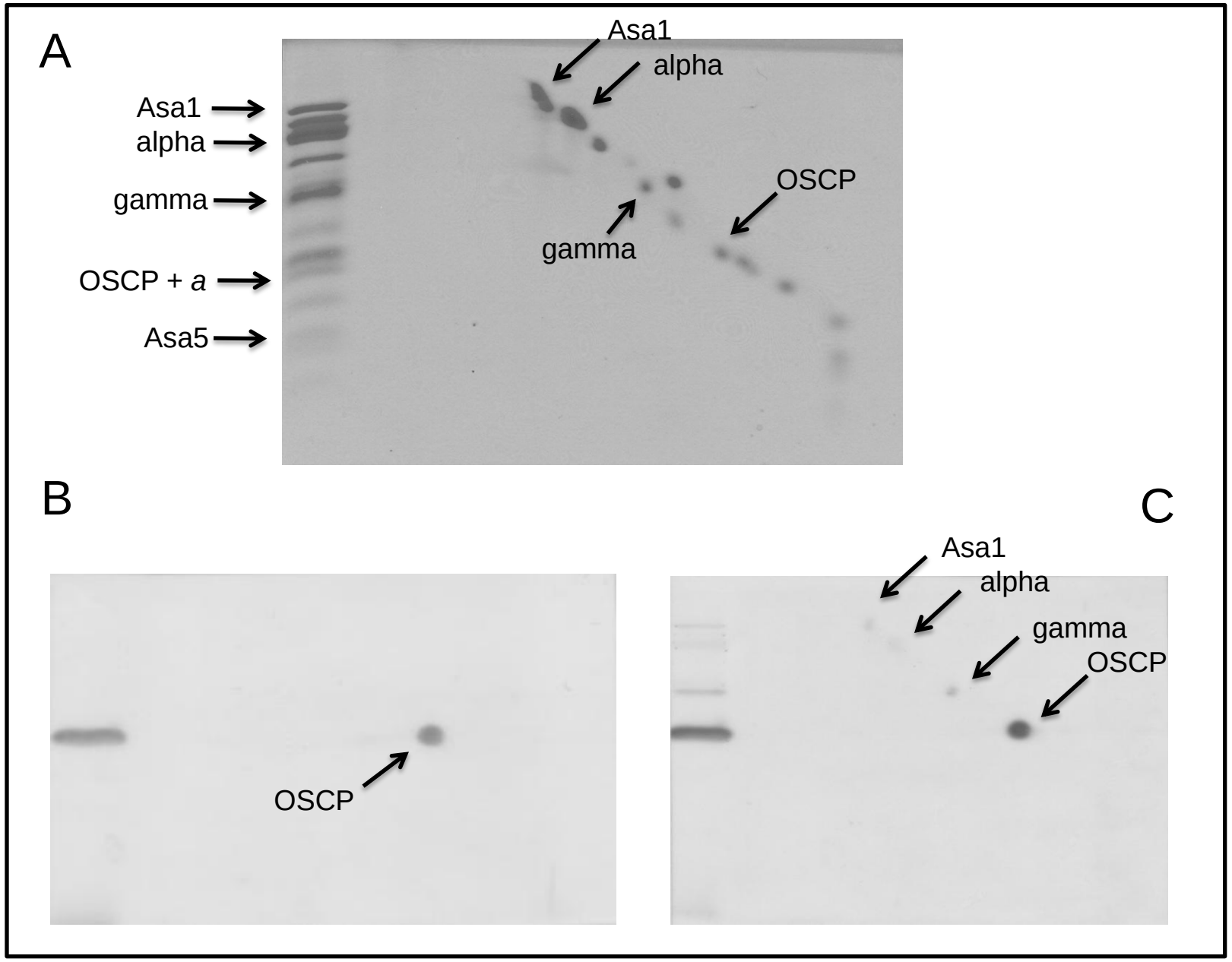

Figure 4

Figure 05

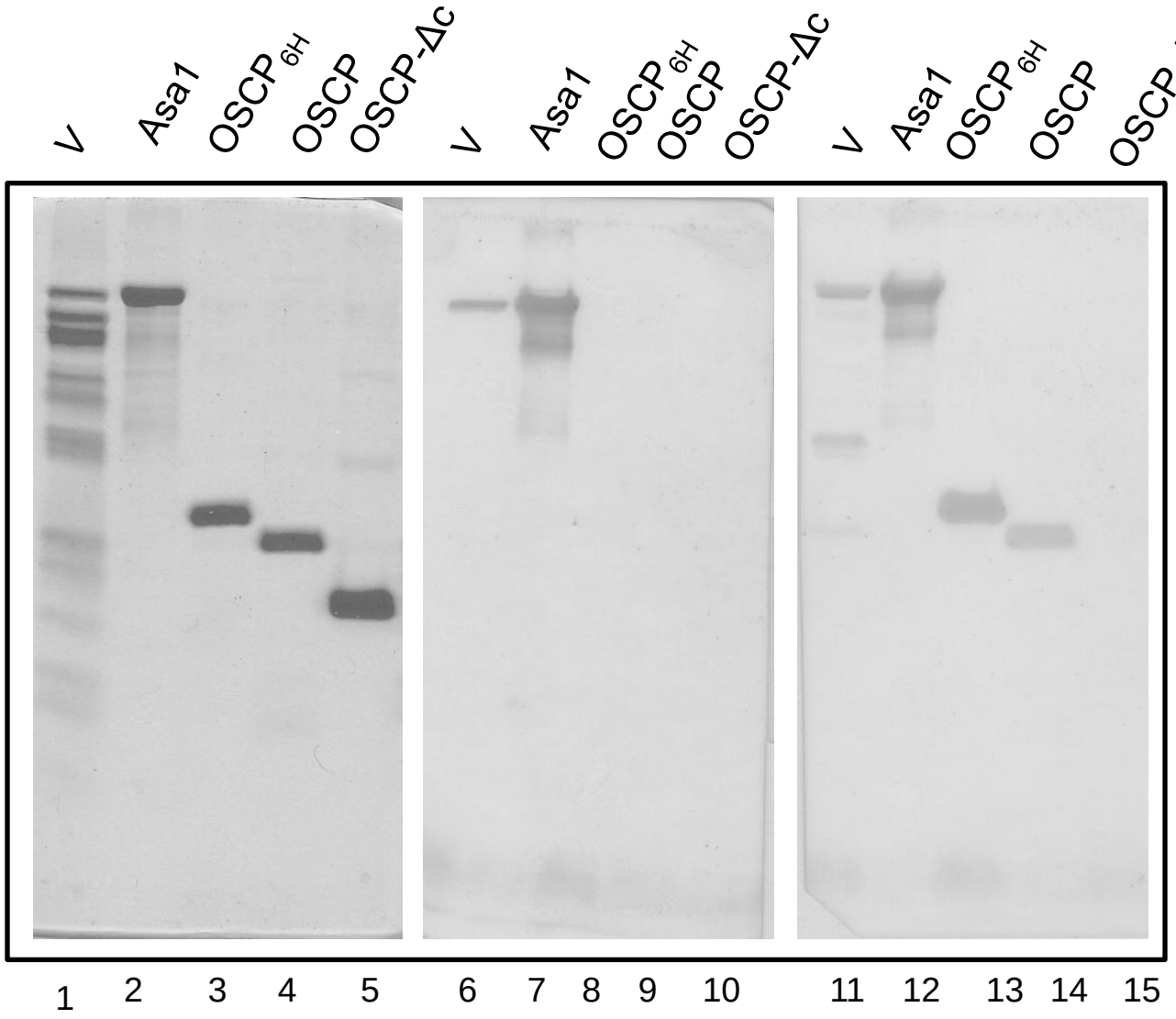

Figure 5

Figure 06A

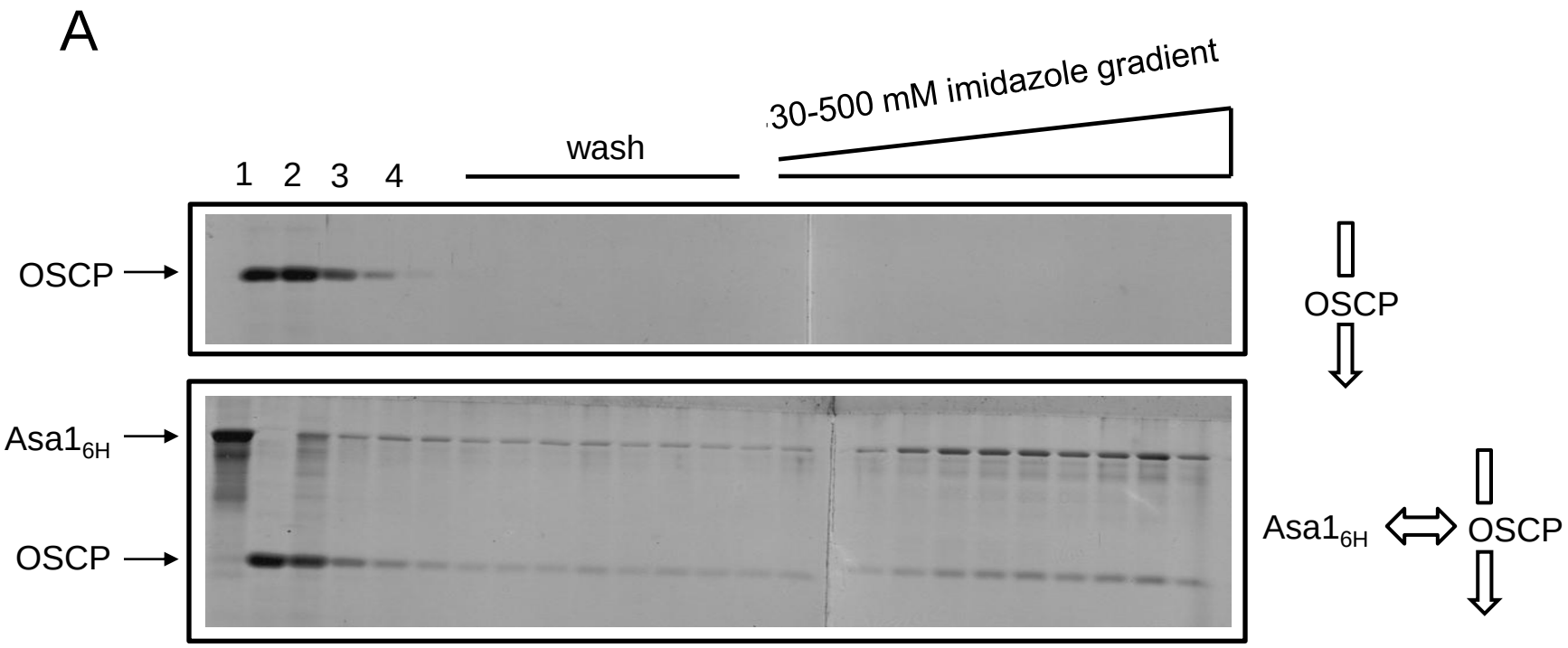

Figure 6

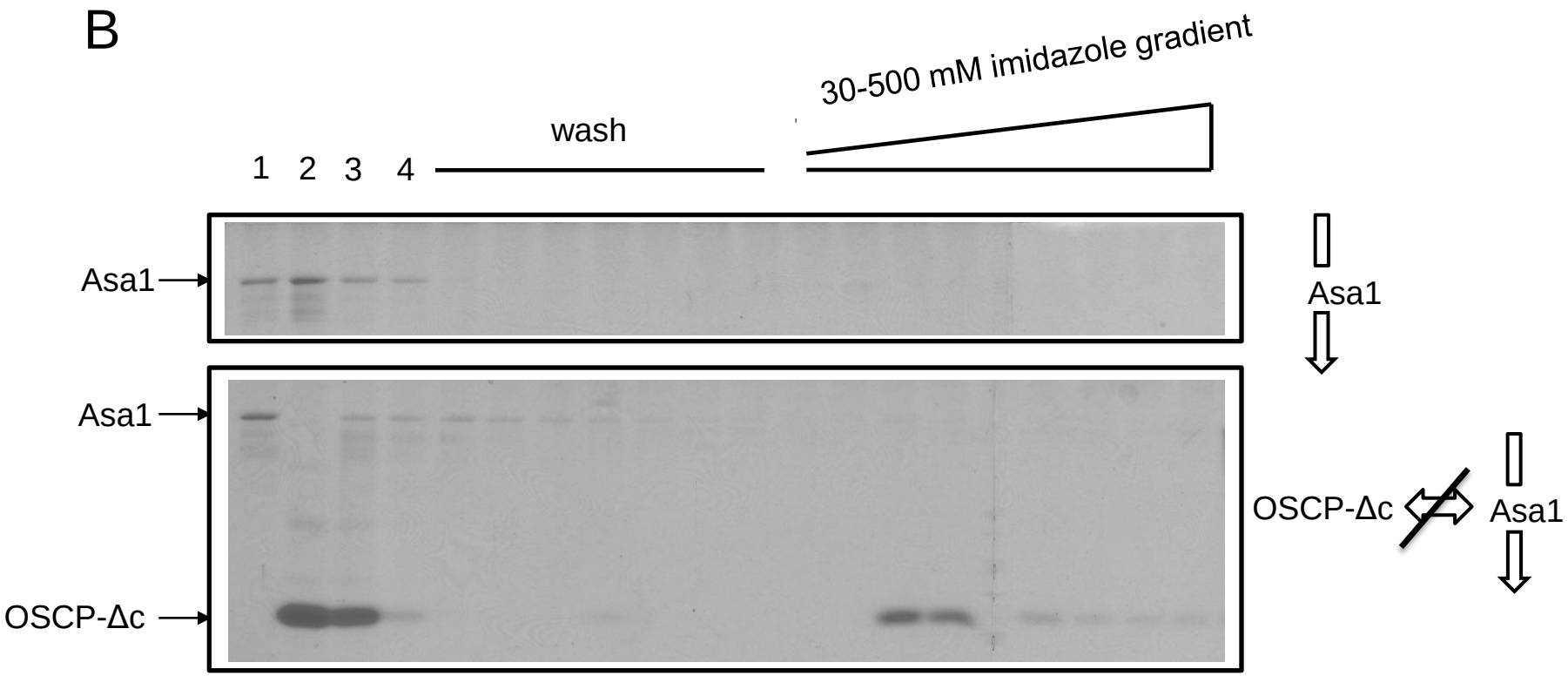

Figure 6 (continued)

Figure 07A

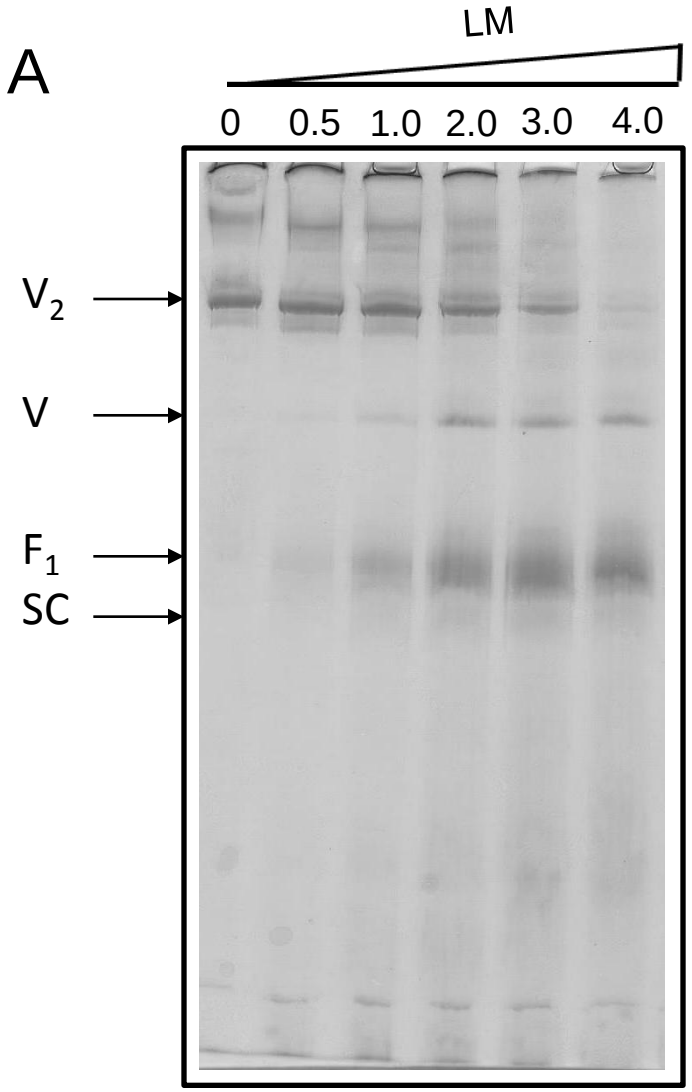

Figure 7

Figure 07B

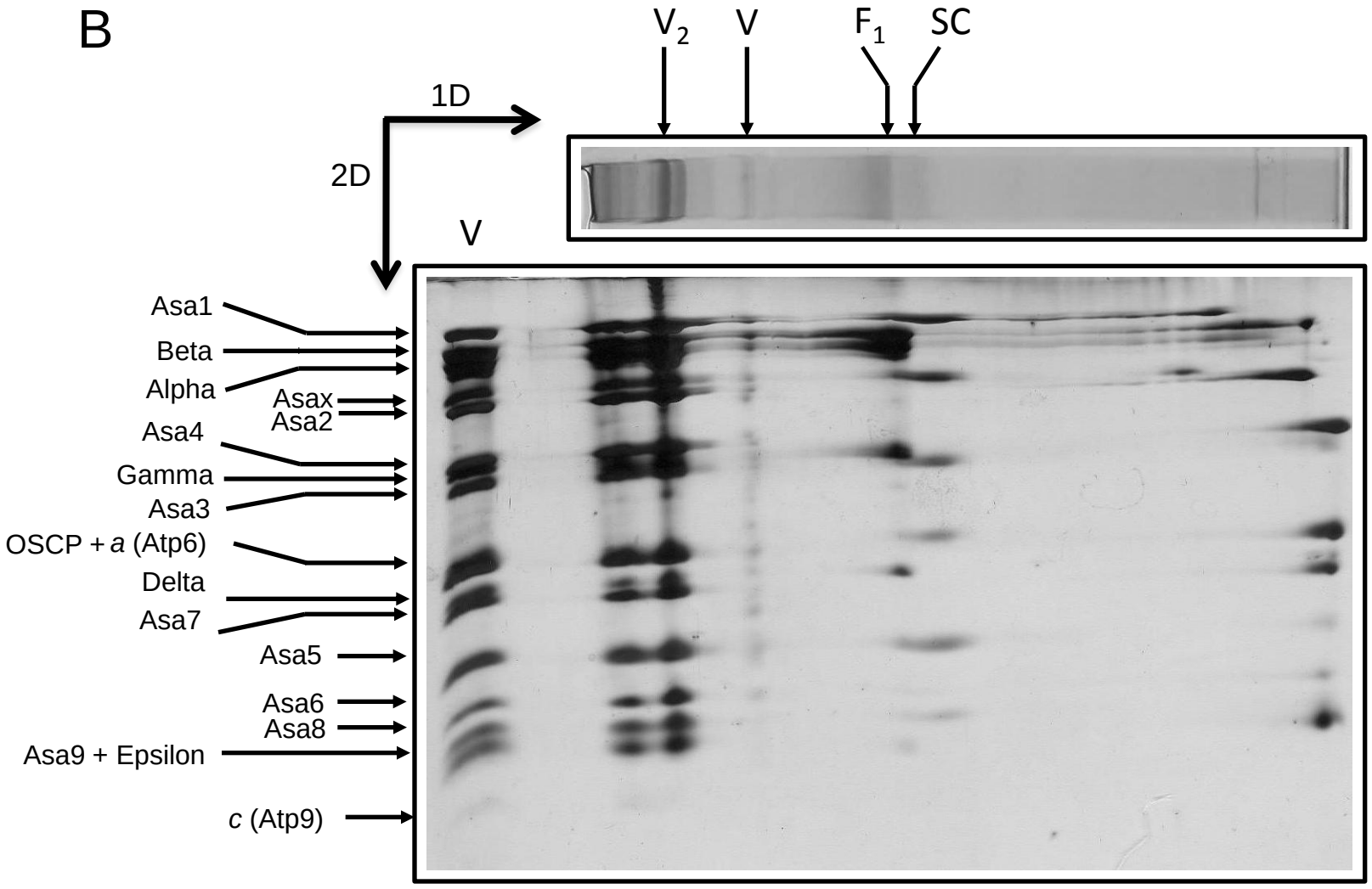

Figure 7 (continued)

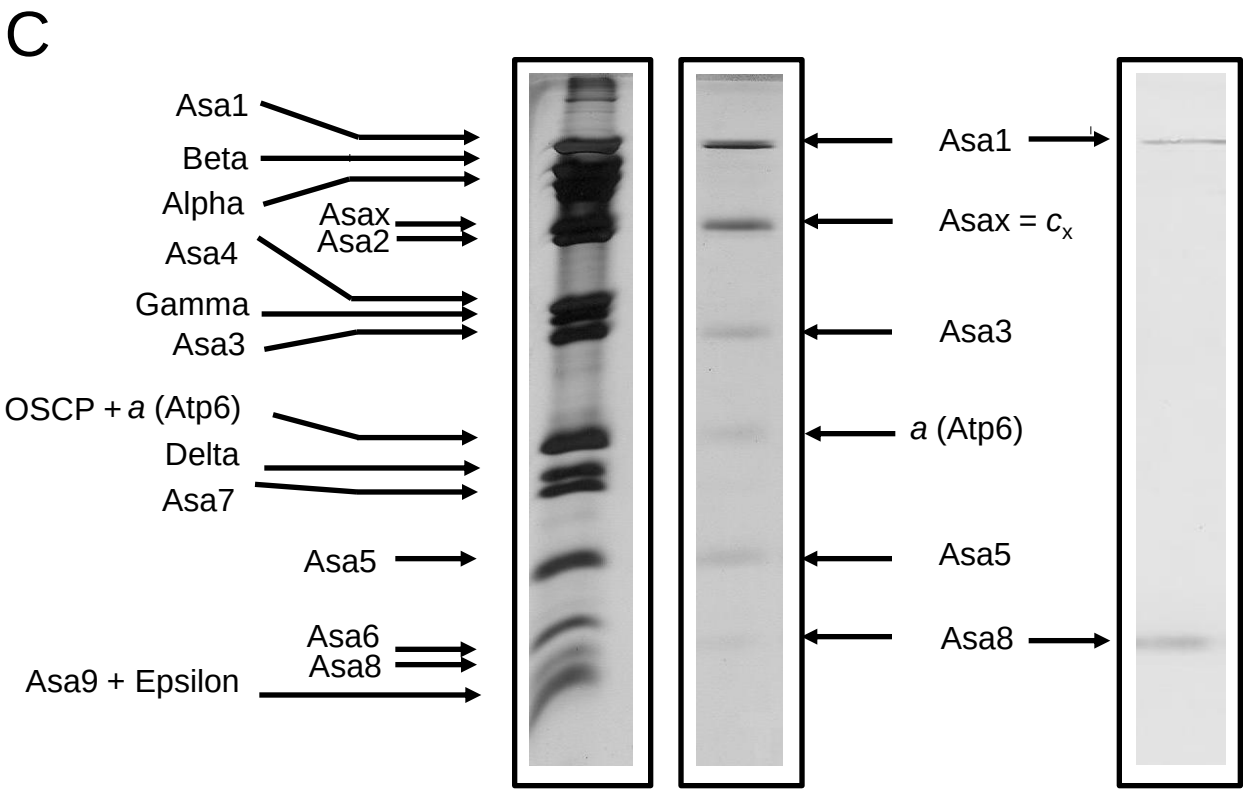

Figure 7 (continued)

Figure 08A

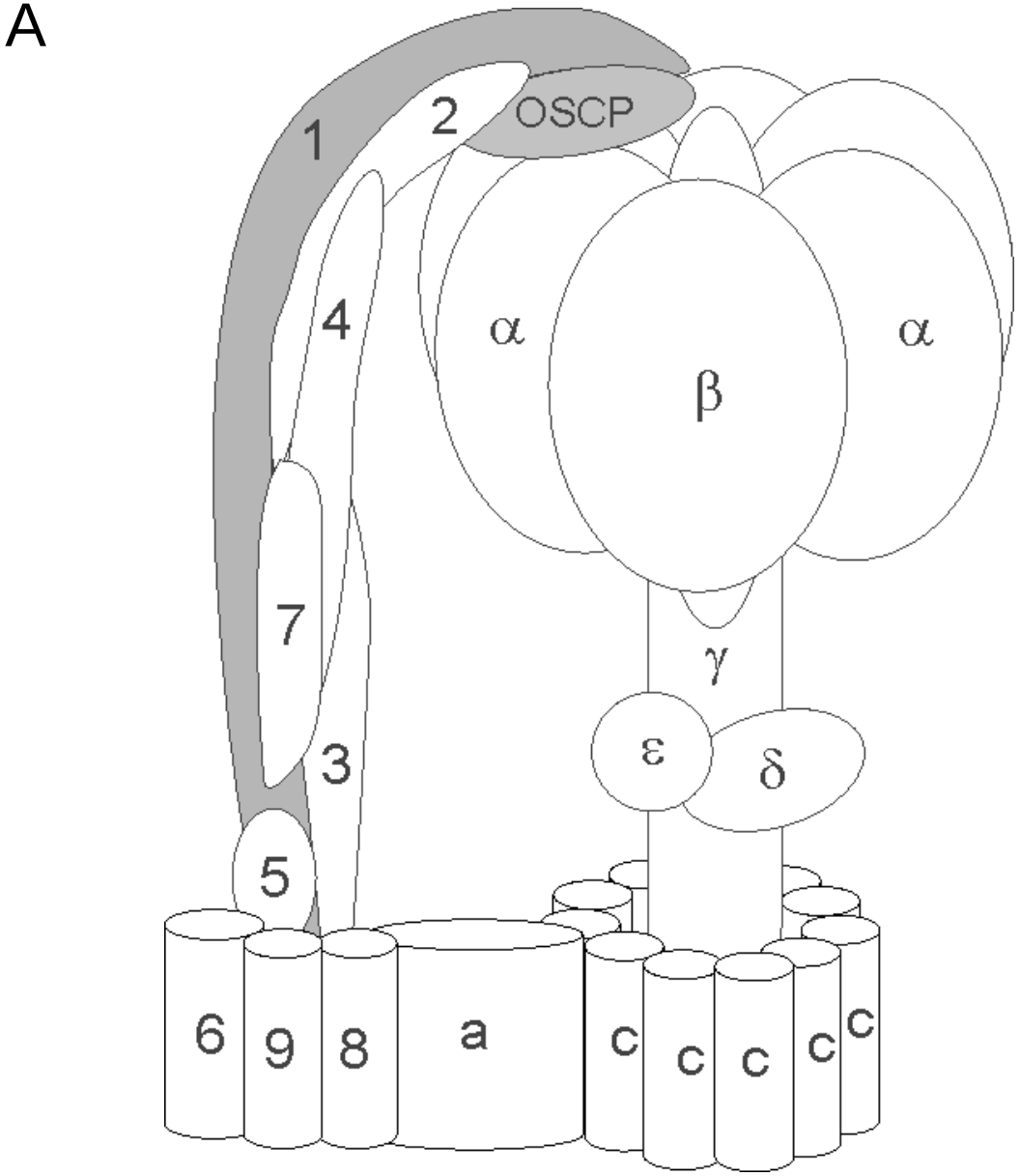

Figure 8

Figure 08B

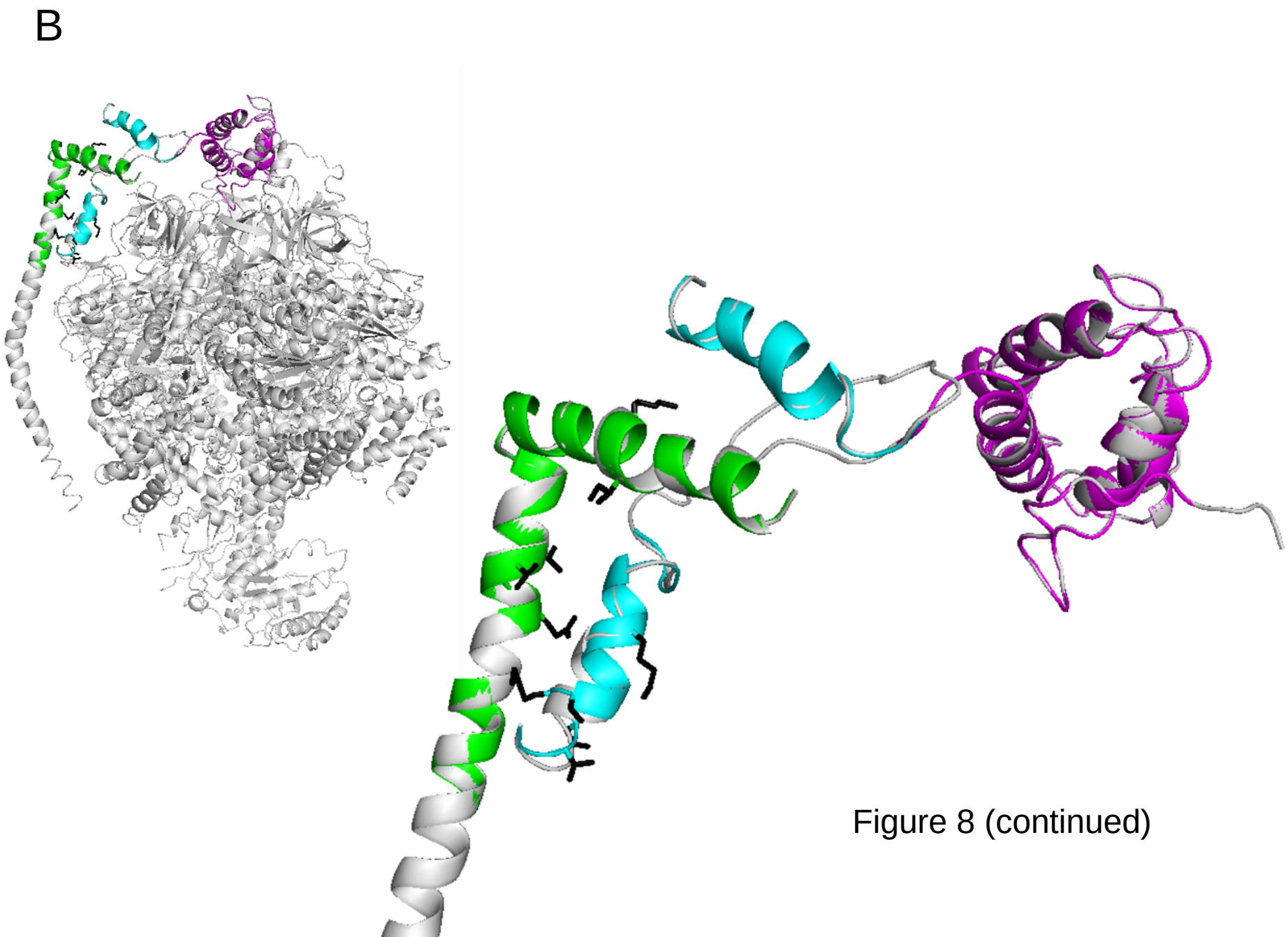

Figure 8 (continued)

Supplementary Material (for online publication)

Click here to download Supplementary Material (for online publication): FigureS01.ppt

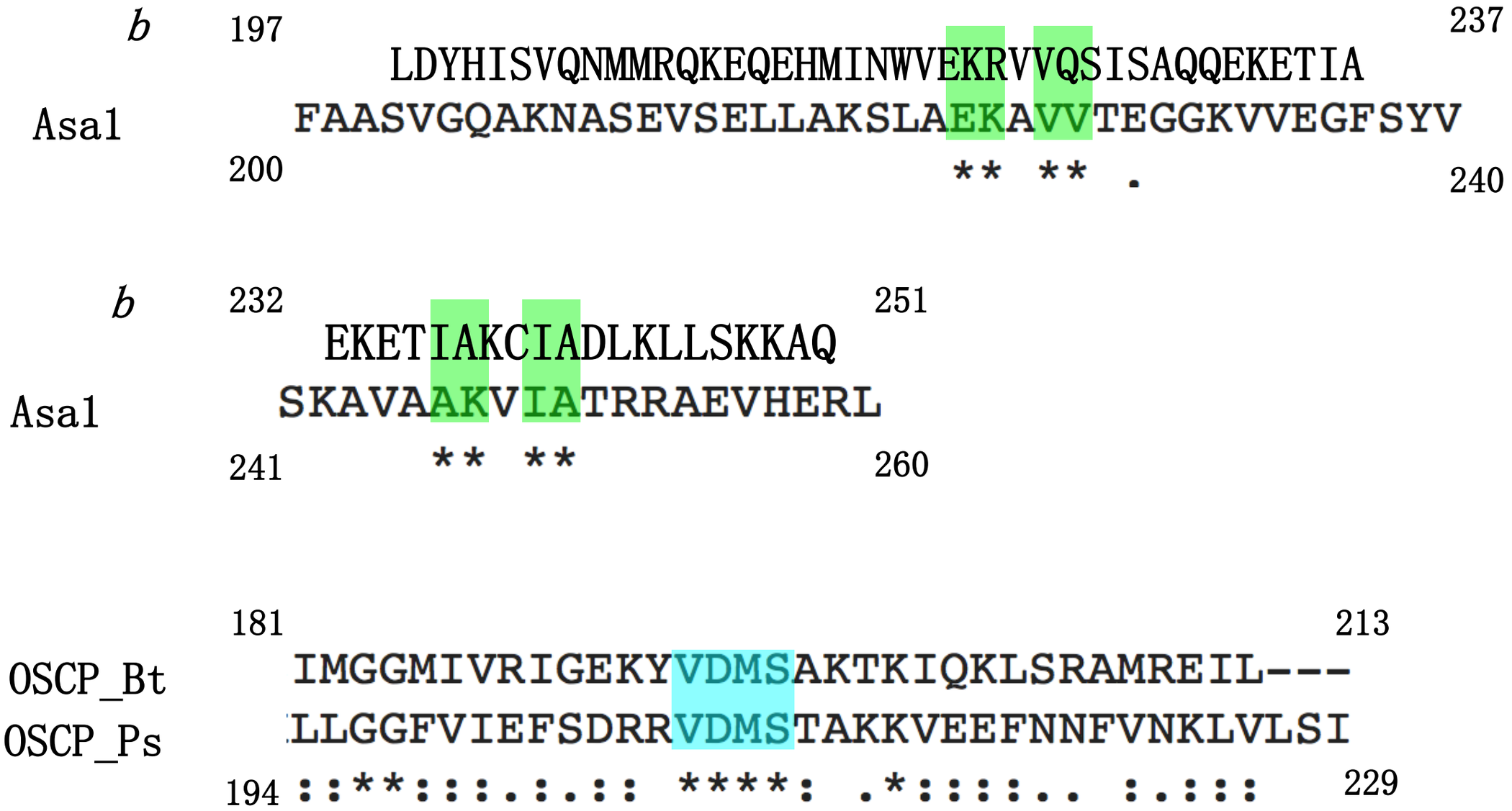

Supplementary Figure 1

Supplementary Material (for online publication)

Click here to download Supplementary Material (for online publication): FigureS02.ppt

Supplementary Figure 2

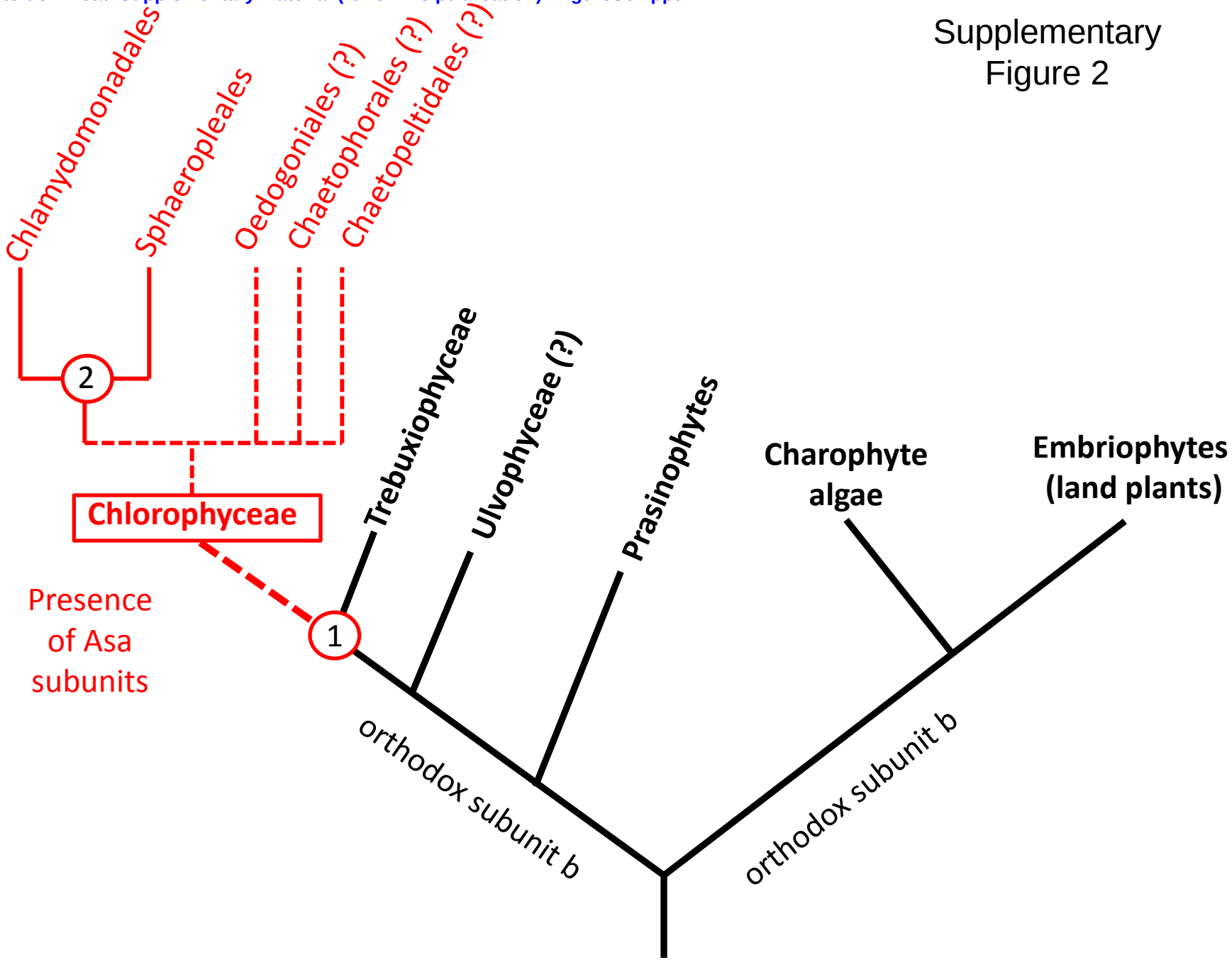

Supplementary Material (for online publication)

Click here to download Supplementary Material (for online publication): FigureS03.docx

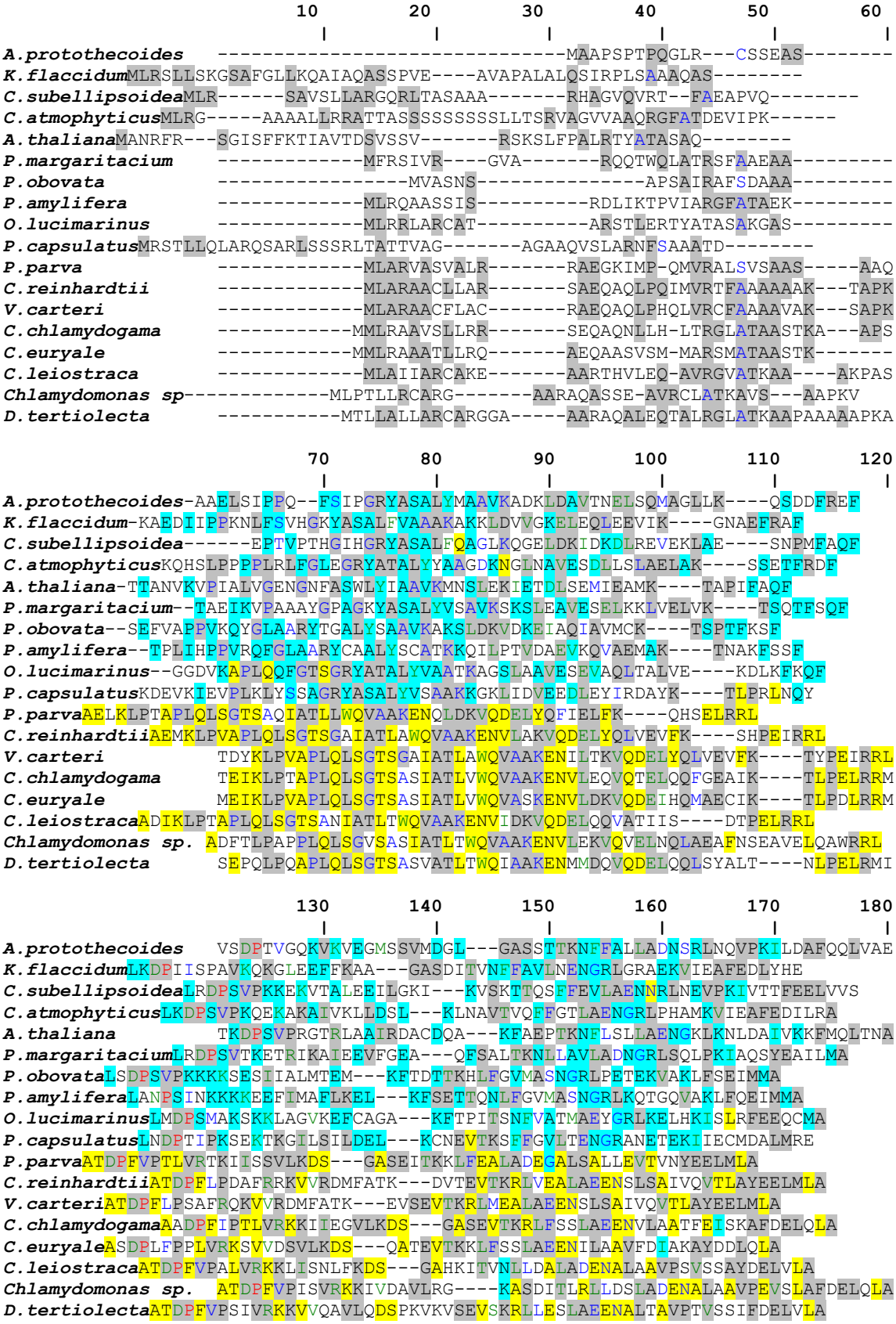

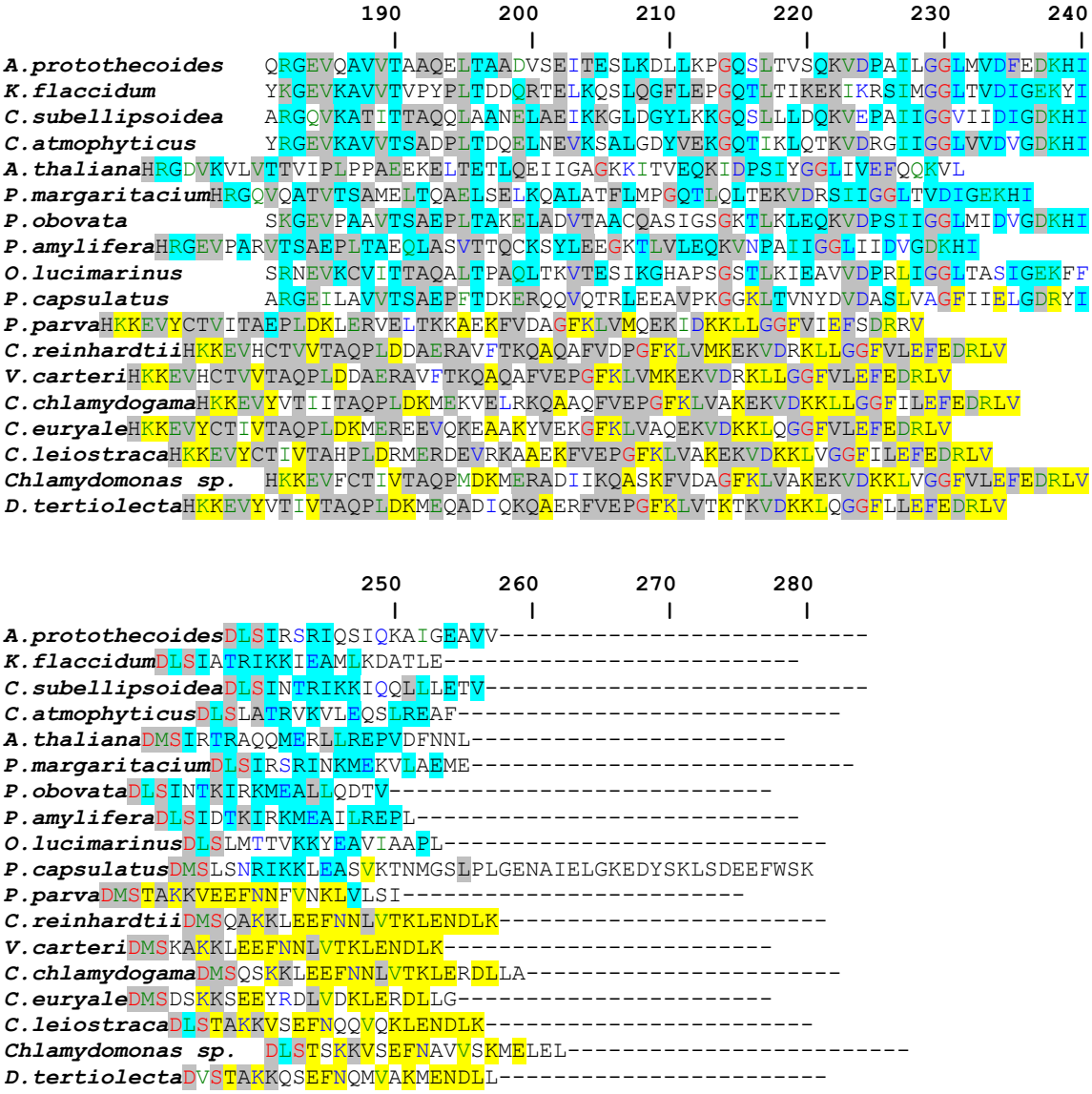

Supplementary Figure 3

***Conflict of Interest**

Click here to download Conflict of Interest: ConflictInterests.pdf